CHAPTER

23

Nanodimensional materials: an approach toward the biogenic synthesis

Tahmeena Khan[1], *Qazi Inamur Rahman*[1], *Saman Raza*[2], *Saima Zehra*[2], *Naseem Ahmad*[1] *and Azamal Husen*[3,*]

[1]**Department of Chemistry, Integral University, Lucknow, Uttar Pradesh, India** [2]**Department of Chemistry, Isabella Thoburn College, Lucknow, Uttar Pradesh, India** [3]**Wolaita Sodo University, Wolaita, Ethiopia**

***Corresponding author. e-mail address:** adroot92@gmail.com

23.1 Introduction

Nanotechnology has appeared as a dynamically evolving discipline of scientific interest that includes materials that have at least one dimension ranging between 1 and 100 nm. The concept of biogenic synthesis has been explored widely to meet sustainable development goals (Husen, 2019, 2020; Husen and Jawaid, 2020; Siddiqi and Husen, 2016a,b). It has been considered that nanotechnology is one of the most promising fields catering to the sustainable use of chemistry without jeopardizing environmental health and well-being. The field of nanotechnology has a lot of potential and myriad applications because of its multidisciplinary nature (Husen and Siddiqi, 2014; Husen, 2020, 2022; Kumar et al., 2021a,b; 2022; Sharma et al., 2021, 2022; Jin-Chul et al., 2021; Alle et al., 2022). Nanotechnology merges disciplines like chemistry, physics and biology to synthesize nanoparticles (NPs) with unique properties and dimensions. The properties of NPs may be enhanced by infusing noble metals like gold (Au), silver (Ag), or platinum (Pt) (Gul et al., 2021). Since the environmental deterioration is taking at a very fast rate, hence there is a persuasive need to develop and synthesize cost-effective and environment-friendly NPs, which has been realized with the advent of green synthesis (Mishra et al., 2019; Joshi et al., 2019; Bachheti et al., 2019a,b). For this purpose, several biological systems are presently employed and plant-based synthesis is now used extensively for the environment-friendly production of NPs.

Advances in Smart Nanomaterials and their Applications
DOI: https://doi.org/10.1016/B978-0-323-99546-7.00009-4

© 2023 Elsevier Inc. All rights reserved.

In the recent past, several plants (or their parts and products) such as *Anacardium occidentale* (Chandra and Khan, 2020), *Calotropis gigantean* (Kumar et al., 2020), *Citrus lemon* (Nabi et al., 2022); *Hibiscus rosa sinensis* (Buarki et al., 2022); *Hisbiscus sabdariffa* (Zangeneh and Zangeneh, 2020), *Malus domestica* (Kazlagic et al., 2020), *Nigella sativa* (Aygun et al., 2020a,b), *Phoenix dactylifera* (Rambabu et al., 2021), *Syzygium aqueum* (Manjare and Chaudhari, 2020), among others, have been effectively utilized for efficient and rapid biogenic NPs synthesis (Fig. 23.1). Further, biogenic NPs synthesis depends on various growth factors, for instance, the concentration of plant extract or biomass, the concentration of salt, incubation or reaction time, temperature and pH of the solution. Hence, standardization of these growth factors is important in obtaining the desired size and shape of NPs for their maximum exploitation and application. The most commonly used techniques for the characterization of NPs are UV-vis spectroscopy, transmission electron microscopy (TEM), scanning electron microscopy (SEM), X-ray diffraction (XRD) and Fourier transform infrared spectroscopy (FTIR). These techniques facilitate the determination of size, shape, structure, crystal orientation and phases, composition, surface modification and surface chemistry of NPs.

While using NPs, toxicity considerations are important to assure that the NPs are safe and nonhazardous (Fadeel and Garcia-Bennett, 2010). Synthesis and or fabrication of metals and metal-oxide NPs may pose threat to human beings and therefore it becomes crucial to assess cellular alternations and DNA injury and oxidative stress to the tissues and genotoxicity. The metal-based NPs must also exhibit chemical inertness if they are being used for implants. Overall, the objective of this chapter is to present the current information on plant-based (biogenic) NPs synthesis and its beneficial applications.

23.2 Biogenic synthesis of nanoparticles

The biogenic NPs synthesis and or fabrication relies on an environmentally free solvent (water or ethanol), a nontoxic reducing and stabilizing agent whereas the conventional chemical procedures involve toxic and hazardous substances posing a threat to the environment (Nath and Banerjee, 2013; Husen and Siddiqi, 2014). The biogenic synthesis may use fungi, algae, bacteria, or plants, of which plants have been widely used for the synthesis of NPs for large-scale production. Different plant parts like leaves, fruits, roots, stems and seeds can be employed to extract the NPs of well-defined size, composition and shape (Narayanan and Sakthivel, 2011; Husen et al., 2019; Husen, 2019, 2020). Plants are abundant in natural phytochemicals which may also act as stabilizing and reducing agents for the synthesis of NPs. Synthesis using plants and associated products is not only eco-friendly but also easy to manage. In addition, the NPs so produced are rich in biomolecules like phenols, tannins, flavonoids, etc., which prevent their interaction with atmospheric oxygen (Chouhan and Mandal, 2021) thereby enhancing their stability. Plant-derived NPs may also be stored over a longer period and are not easily oxidized. Waste materials like banana and lemon peels and dried leaves are routinely used for the green synthesis of NPs. These NPs can also be fabricated with noble metals like Ag, Au and Pt. Silver nanoparticles (AgNPs) are easily derived from plants (Majeed et al., 2018) and require a silver salt solution and a reducing agent. Polysaccharides, vitamins, amino acids, phenolics, alkaloids and terpenes may be used as reducing and stabilizing agents (Aslam et al., 2021). Other than that gold nanoparticles

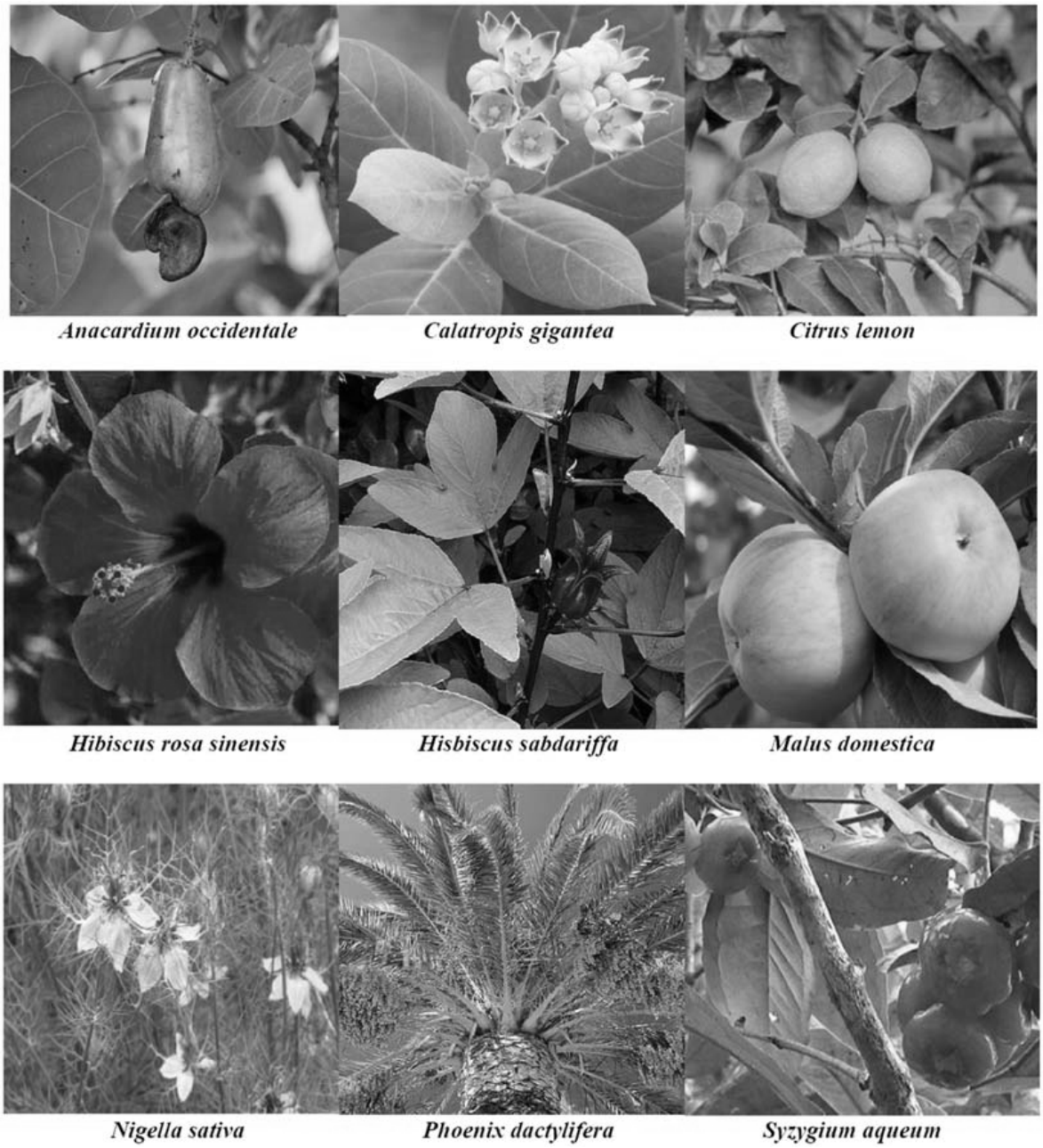

FIGURE 23.1 Some of the recently used plants for efficient and rapid biogenic nanoparticles synthesis.

(AuNPs) are also easy to synthesize, have flexible surface functionalization and hold potential as therapeutic agents (Amina and Guo, 2020). Phytoconstituents including phenols, flavonoids and proteins, etc., may have an important role in the reduction of gold ions and the synthesis of gold-based NPs. Zinc oxide (ZnO) based nanoparticles (ZnO NPs) have also received considerable attention because of their use in cosmetics and electronics etc. ZnO NPs are derived from flowers, seeds and leaves and exhibit a high exciton binding energy

(60 meV) and a bandgap of 3.37 eV making them good semiconductors (Sanakouser et al., 2022). Copper (Cu) is a relatively cheap metal and is used to derive Copper nanoparticles (CuNPs) by reducing the aqueous solution of copper ions using plant extracts CuNPs are also important because of their easy availability and high electrical conductivity (Tiwari et al., 2016). Ni, Mn, Pd, Ce and Pt-based NPs are also reported with an array of applications in different fields (Hano and Abbasi, 2021).

23.3 Mechanism of the synthesis of nanoparticles

Plants are a storehouse of a variety of bioactive substances like alkaloids, flavonoids, and steroids, etc. which act as reducing agents. Plants like *Acalypha indica*, *Ficus benghalensis*, *Zingiber officinale*, *Plumbago zeylanica*, *Centella asictica*, *Parthenium hysterophorus*, *Sapindus rarak*, *Passiflora foetida*, and so on have been explored to synthesize NPs through a one-step process. The general requirements for the plant-based synthesis of NPs are reducing and capping agents, metal salt, and solvent and the steps involved in the synthesis are nucleation, growth, aggregation, stabilization and characterization. Amino acids, citric acid, flavonoids, tartaric acid and secondary plant metabolites are used as reducing agents. The reduction potential of the metal also affects the reduction. A metal with a positive reduction potential can be reduced at a faster rate. At a low reduction rate, the nucleation and growth are in equilibrium (Lee et al., 2009). A previous study reported a one-step synthesis of Au-PdNPs where the reduction rate was slow with the reduction potentials of Pd^{2-}/Pd and Au^{4-}/Au being 0.59 and 0.99 eV respectively (Zhang et al., 2015). The difference in the redox potential between the two metals was responsible for the synthesis of core-shell NPs. In another study, it was established that terpenoids from geranium leave helped in the reduction of Ag^{+} ions (Shankar et al., 2003) which later on get oxidized to carbonyl groups. Similarly, tartaric acid was recognized as a capping medium for the bioreduction of gold particles as obtained from tamarind leaf broth (Ankamwar et al., 2005). Another study reported the adsorption of silver by alfalfa roots as Ag(0) and how it is being transmitted to the shoots without a change in its oxidation number (Gardea-Torresdey et al., 2003). The characterization of the NPs was done through SEM, TEM, XRD, UV-Vis and FTIR spectroscopic techniques. The SEM and TEM are employed to assess the shape, size and aggregation of the NPs (Xiao et al., 2016), whereas with the help of EDX the composition and distribution of NPs can be done. The UV-Vis spectroscopic technique is used to investigate NPs based on the average size and aggregation (Davids et al., 2021). The signal in the UV-Vis spectrum is based on the absorption of plasmas by free electrons adhered on the surface of NPs leading to the interaction with the electromagnetic field and shifting towards the higher wavelength. FTIR and XRD are used to determine the structural characteristics and crystallinity of the NPs.

23.4 Factors affecting the synthesis of plant-based nanoparticles

Several factors such as the concentration, pH, incubation time and temperature of the plant extract and or biomass affect the NPs preparation methods. These factors control the

shape and size of NPs during biogenic synthesis. They are discussed in the following subheadings.

23.4.1 pH-dependent effect

Past studies have shown that the size of the AgNPs increases as the pH is decreased (Muthu and Priya, 2017). It was found that the intensity of the surface plasmon resonance (SPR) increased as the pH varied from 3 to 9. The alkaline pH enhanced the reduction and stabilizing potential of the leaf extract of *Ficus hispida*. Another study to synthesize AuNPs from *Avena sativa* extract showed that the size of the NPs was proportional to the pH (Armendariz et al., 2004). Diverse-shaped AuNPs were obtained at pH 8 from the leaf extract of *Angelica archangelica*, *Hypericum perforatum* and *Hamamelis virginiana* in the size range of 4−8 nm (Pasca et al., 2014). A study showed that the color of the AuNPs also depended on the pH. A purple color was formed at pH 7 which became fluorescent at pH 10 (Dhamecha et al., 2016). It has also been reported that the reduced zeta potential of AgNPs was negative in highly acidic pH showing their stability in alkaline pH with smaller size. Nearly spherical NPs were formed at pH 8 having a size diameter of 20 nm. *Zizyphus xylopyrus* bark extracts were used for AgNPs synthesis and reported that the optimum condition is silver nitrate solution at 10 mM; and the alkaline initial pH of 11 facilitates SPR peak of high intensity, showing increased fabrication of AgNPs. Thus, the acidic medium suppressed the production of AgNPs, whereas the basic medium enhanced it (Maria et al., 2015). Ghodake et al. (2010) used pear fruit extract-assisted room-temperature biosynthesis of gold nanoplates. They found that the alkaline condition was more effective for triangular and hexagonal nanoplates, while the structures of these nanoplates were barely detected at acidic pH.

23.4.2 Role of temperature

The literature survey reveals that the size of NPs is negatively proportional to the temperature. A reported that at room temperature (27°C), the mean size of the NPs was 49.91 nm, which decrease with the increase in temperature and reached up to 33.61 nm at 45°C (Lee et al., 2019). A study reported the extraction of AgNPs from Olive leaf (Khalil et al., 2014). As the temperature increased, $Ag+$ ions reduced at a faster rate and at the same time uniform nucleation took place leading to a reduction in the NPs' size. As the temperature rose, the rate of reduction increased, whereas the secondary reduction ceased over the surface of predetermined nuclei (Song and Kim, 2009). Polydispersed particles in the size range of 5−300 nm were obtained at a lower temperature, as reported by another study (Song and Kim, 2009). Upadhyay and Verma (2014) have shown that reaction time is temperature dependent for AgNP synthesis from potato extracts. A change from room temperature to 60°C reduced the reaction time from 16 hours to 15 minutes, and produced spherical NPs with an average size of 61 nm. Effect of temperature on the rate of reaction for AgNP synthesis from *Dioscorea bulbifera* tuber extract has shown the maximum rate of reaction at 50°C (Ghosh et al., 2012). Similar conclusions were drawn while producing AgNPs using *Pulicaria glutinosa* extract (Khan et al., 2013) and *Solanum xanthocarpum* berry

extract (Amin et al., 2012). Sun et al. (2014) used tea leaf extract for AgNP synthesis and produced spherical AgNPs of 91, 129 and 175 nm at 25°C, 40°C and 55°C, respectively. The increase in particle size was ascribed to an increase in the rate of reduction at higher temperatures which further enhanced the particle size. Dubey et al. (2010) reported that an increase in temperature from 25°C to 150°C leads to an increase in the sharpness of absorption peaks for both AgNPs as well as AuNPs in *Tanacetum vulgare* fruit extract. Phillip (2009), and Dwivedi and Gopal (2010) have reported that the high temperature also increases the rate of reaction, which increased NPs synthesis.

23.4.3 Incubation period

The incubation reaction time influences nanoparticle synthesis greatly. A study reporting the synthesis of AgNPs from *Jatropha curcas* showed that the intensity of the SPR peak increased with the increase in reaction time, and after 4 hours of incubation two SPR peaks were obtained (Bar et al., 2009). Another study showed the dependence of the NPs' size on the contact time (Philip, 2011). Similar observations were made in another study with *Rosa damascene* to synthesize AuNPs and AgNPs (Ghoreishi et al., 2011). Dubey et al. (2010) used *T. vulgare* fruit extract for AgNPs and Asynthesishesis. In this experiment, the reaction started within 10 minutes, and an increase in the incubation time led to the sharpening of peaks for these NPs. In another experiment, *Rosa* hybrid petals extract was used (Noruzi et al., 2011). They noticed a higher rate of reaction in comparison to previous studies, as the AuNP synthesis process was finished within 5 minutes (Noruzi et al., 2011). However, using the *Terminalia chebula* plant extracts, Kumar et al. (2012) produced gold NPs in 20 seconds only.

23.4.4 Plant biomass concentration

This is another crucial growth factor for optimum NPs production. The NPs synthesis may occur when a suitable precursor concentration is available in a suitable range for nucleation. The reducing and capping agent availability governs whether the metal precursors could be reduced and ultimately participate in NPs fabrication. Thus, plant biomass concentration at the time of synthesis cannot be ignored, as it facilitates the amount of reduction and stabilization employed by the active biomolecules which usually influence the outcome. In an experiment, *Citrus limon* aqueous extract use AgNPP production and it was noticed that with increasing the mixing ratio of metal solutions and plant biomass, a sller size of NPs was formed. This could be due to the increased amount of electron-rich bioreducing agents once a higher concentration of plant biomass was used in the reaction medium (Prathna et al., 2011). As the plant extract concentration was increased, it increased the electron density as charged groups in the reductants. Possibly, this facilitated the free electrons of the metallic cluster within a small volume and intensified the surface charge on the metallic clusters. This surface charge might exert a repulsive force that could decrease the particle size. Dubey et al. (2010) used the aqueous extract of *Sorbus aucuparia* leaf for the synthesis of AgNPs and AuNPs. Dubey et al. (2010) noticed an increased particle formation and a reduced size of both the silver and gold nanocolloids

when the amount of extract was increased. Similarly, an increase in the amount of the *Chenopodium album* leaf extract caused a decrease in particle size (Dwivedi and Gopal, 2010). During the biosynthesis of gold NPs with the help of *Sapindus mukorossi* extract, few aggregations and heterogeneous structures were observed at a lower (15%) concentration, while spherical NPs and more dispersion occurred at a higher (45%) concentration (Reddy et al., 2012).

23.5 Some important plant-derived nanoparticles

23.5.1 Metal nanoparticles

23.5.1.1 Silver nanoparticles

AgNPs have distinct properties and have medical and industrial utility (Jiang et al., 2004). They have a high surface/volume ratio and phytoconstituents like alkaloids, phenolic compounds, flavonoids and, terpenoids may reduce silver ions to NPs (Parlinska-Wojtan et al., 2016). Plants like *Tribulus terrestris*, *Astragalus tribuloides* have been explored to synthesize AgNPs between the size of 2−6 nm (Sharifi-Rad et al., 2020). *Curcuma* bark extract is another good source of AgNPs (Sathishkumar et al., 2010). Spherical to plate-like AgNPs have been obtained from the leaf extract of *Lonicera japonica* (Kumar and Yadav, 2011). The seed extract of *Syzygium cumuni* seed extract has been explored to synthesize crystalline AgNPs (Banerjee and Narendhirakannan, 2011) and from the latex extract of *Plumeria rubra* (Patil et al., 2012). Vincristine and vinblastine were found to be responsible for the production of AgNPs from *Catharanthus roseus* (Ponarulselvam et al., 2012). AgNPs may be useful in catalysis, however, no specific reaction using ag as a catalyst is known. They are also good antibacterial agents. During the synthesis of AgNPs Ag^+ ions may be precipitated as AgCl (Costa-Coquelard et al., 2008) which can vary in color upon exposure to sunlight. The color change also denotes the chemical composition and size of NPs. Since AgCl settles as precipitates it requires the presence of some reducing agent for Ag^+ ions. In this context, the role of $Na_2S_2O_3$ has been elucidated and it was found that $Ag_2S_2O_3$ would have been formed upon the reaction of $AgNO_3$ with $Na_2S_2O_3$ [Eq. (23.1)]

$$2AgNO_3 + Na_2S_2O_3 \rightarrow Ag_2S_2O_3 + 2NaNO_3 \tag{23.1}$$

Although it has been reported that Ag^+ ions may also react with polysaccharides and amino acids, DNA and RNA for AgNPs, at the same time it is also true that the Ag^+ ions form complex with specific electron donors and require a reducing agent (Shevchenko et al., 1996) [Eq. (23.2)−(23.3)].

$$Ag^+ + 2NRH_2 \rightarrow \left[Ag(RNH_2)_2\right]^+ \tag{23.2}$$

$$2Ag^+ + H_2 \rightarrow 2Ag^+ + 2H^- \text{ Ag-nanoparticle} \tag{23.3}$$

The absorption of $AgNO_3$, $Na_3Ag(S_2O_3)_2$ and $Ag(NH_3)_2NO_3$ and their reduction has been studied in *Brassica juncea*. It was found that the reduction of metals depended on the concentration of metal salts (Haverkamp and Marshall, 2009). The rate at which the AgNPs grow is not dependent on the concentration of salt but the mobility is affected by

the size of the ion. In the case of $Na_3Ag(S_2O_3)_2$ and $AgNO_3$ the availability of Ag^+ ions will be more in the form of $AgNO_3$. However, the rate of deposition of AgNPs from $AgNO_3$ containing small anions is faster than that with large anions like $S_2O_2^{3-}$.

23.5.1.2 Gold nanoparticles

AuNPs find tremendous use as catalysts, in nanoelectronics and as diagnostic agents (Aromal and Philip, 2012). Tea leaf extract has can be employed to synthesize AuNPs (Sharma et al., 2012). Another study reported the synthesis of AuNPs from the root extract of *Morinda citrifolia* in the size range of 8–17 nm (Suman et al., 2014). Spherical AuNPs have been reported from the alcoholic extract of Nyctanthes arbortristis in the size range of 19.8–5.0 nm (Das et al., 2011), similarly, they were also extracted from *Aegle marmelos* leaves with a size range of 4–10 nm (Jha and Prasad, 2011). The peel extract of *Garcinia mangostana* was employed for the synthesis of AuNPs involving the reduction of Au. The anthocyanins, benzophenones and flavonoids found in *G. mangostoma* helped in the reduction, as suggested by the FTIR results. The bark extract of *Mimosa tenuiflora* was also employed to obtain AuNPs at different metallic concentrations (Rodríguez-León et al., 2019). Triangular and hexagonal AuNPs have been reported from $HAuCl_4$ solution and diluted extract having phyllanthin from *Phyllanthus amarus* (Kasthuri et al., 2009) and *Benincasa hispida* seed extract (Aromal and Philip, 2012). During the reduction process, the COOH group acted as a surfactant and was reduced to COO− and adhered to AuNPs, thereby stabilizing it. The biosynthesis of AuNPs depends upon the concentration of plant extract and the metal salt along with the temperature and pH of the solution. The synthesis of AuNPs from *A. sativa* biomass showed different structures of NPs ranging from tetrahedral, hexagonal and decahedral, icosahedral and irregular (Armendariz et al., 2004) with the highest yield obtained at pH 3. The oat biomass showed the ability to bind $AuCl_4^-$ leading to the reduction of AuNPs. They have been obtained from dead leaf tissues of alfalfa. It has been found that plants associated with aroma-producing flavonoids, sugars and alcohols/phenols act as reductants leading to the formation of NPs. They have been produced from dead and live tissue of alfalfa (Gardea-Torresdey et al., 2002), hops (Lopez et al., 2005), fungus (Mukherjee et al., 2002) and algae (Kuyucak and Volesky, 1989).

23.5.1.3 Platinum and palladium nanoparticles

Palladium and platinum have high-density and fabricated NPs have been isolated from plants like *Anogeissus latifolia*, *Cinnamomum camphora*, *Curcuma longa*, *Doipyros kaki*, *Musa paradisica*, *Ocimun sanctum*, *Pinus resinosa* and *P. glutinosa*, etc. The fabricated NPs possess heterogeneous catalytic activity as shown by the Suzuki-Miyaura coupling reaction (Nasrollahzadeh et al., 2015), which is ligand-free and easily conducted in an aqueous medium. PdNPs have been obtained from the leaves of *Hippophae rhamnoids* (Nasrollahzadeh et al., 2015) and characterized by SEM, TEM, XRD and UV-Vis spectroscopic techniques. The polyphenols present in the plant acted as reducing and capping agents. Bimetallic NPs of Au and Pd having core-shell structures have been reported (Xu et al., 2011). Palladium used for the reduction of Au was in turn reduced by adding a mild reducing agent like *Cacumen platycladi* leaf extract. The root extract of *Euphorbia condylocarpa M. bieb* was used for the green synthesis of Pd/Fe_3O_4NPs

(Nasrollahzadeh et al., 2015). The flavonoids present in the extract acted as reducing agents for the metal ions. Barberry fruit extract was used for the biosynthesis of PdNPs. Vitamin C present in the fruit reduced the metal ions to NPs with an average size of 18 nm (Nasrollahzadeh et al., 2016). *Salvadora persica* root extract rich in polyphenols has been used to obtain PdNPs. The polyphenols were found to act as bioreductant and stabilizing agents and NPs with an average size of 10 nm were obtained upon heating at 90°C (Khan et al., 2013). The bark extract of Cinnamomum zeylanicum which is rich in constituents like linalool, ethyl cinnamate, eugenol and cinnamaldehyde has a rich aroma has convert Pd ions to PdNPs (Muthuswamy et al., 2008). Fabricated and crystalline PtNPs having a size range between 30 and 60 nm were obtained from tea extract and the polyphenols found in the extract acted as reducing and capping agents (Sheny et al., 2013). The NPs were found to have a face-centered cubic structure. The TEM images showed that the NPs were flower-shaped (Porcel et al., 2010). The leaf broth of *O. sanctum* was used for the biosynthesis of PtNPs at 100°C (Soundarrajan et al., 2012). The reduction of the metal ions was identified by a color change from yellow to brown and finally black. Ascorbic acid and terpenoids present in the extract acted as reducing and stabilizing agents with an average size of 23 nm. The energy dispersive absorption X-ray spectroscopy (EDAX) showed 71% Pt while XRD indicated the presence of PtO_2, $K_2[PtCl_4]$, Pt and $PtCl_2$. Leaf extract of *D. kaki* has been utilized for the extracellular synthesis of PtNPs at 95°C using $H_2PtCl_6.6H_2O$ (Song et al., 2010). The size of the NPs was found to decrease with the increase in temperature. The biosynthesis of PtNPs from *Azadirachta indica* extract was done to obtain NPs of size between 5 and 50 nm (Thirumurugan et al., 2016). The fabrication of Pt increased with the increase in reaction temperature. The terpenoids found in *A. indica* acted as reducing agents. PtNPs have been obtained from *Medicago sativa* and *B. juncea* plant biomass.

23.5.1.4 Zinc and copper nanoparticles

Zinc nanoparticles (ZnNPs) have been in consideration owing to their cost-effectiveness, large surface area and antimicrobial properties (Kumar et al., 2013). Phytochemicals like polyphenols, saponins and terpenoids act as reducing and stabilizing agents and they have been obtained from different plant parts like root, stem, leaf, fruit and seed. These phytoconstituents are responsible for the reduction of metal ions to zero oxidation state which can further be calcinated to their oxide. Zn^{2+} ions may also interact with polyphenols to form a complex. Plants from the families of Fabaceae, Rutaceae, Solanaceae and Lamiaceae, etc. are mostly employed for the synthesis of ZnNPs (Kumar et al., 2013). The floral extract of *Cassia auriculate* was made to react with $Zn(NO_3)_2$ solution leading to the formation of ZnNPs (Ramesh et al., 2014) having a particle size between 110 and 280 nm. CuNPs have emerged as antimicrobial, antioxidant and antifouling agents when infused in coatings and textiles (Thiruvengadam et al., 2019). They also act as heat transfer fluids, sensors and gas-sensing agents (Sharma et al., 2015). Spherical CuNPs with a size of 23 nm have been obtained from the flower extract of *Millettia pinnata* (Din et al., 2017). The UV-Vis analysis confirmed the reduction of copper acetate to CuNPs. Proteins, flavonoids and carboxylic acid were found to be responsible for the reduction of Cu^{2+} ions to CuNPs. *Magnolia kobus* leaf extract was used to obtain spherical CuNPs of a size diameter between 50 and 250 nm (Lee et al., 2013). With the increase in temperature yield of CuNPs increased. CuNPs have been fabricated from copper sulfate and *Eucalyptus*

sp. Leaf extract at ambient temperature (Kulkarni et al., 2015). A slight change in the pH was obtained upon adding the leaf extract resulting in the color change. Phenols, amino acids and amines were responsible for the reduction and capping. Leaf extract of *A. indica* was used to synthesize CuNPs and the effect of temperature, pH and concentration of the salt on the conversion rate of CuNPs was studied (Kulkarni et al., 2015). Ultra-small CuNPs of the size range of 2.90 nm has been obtained from lemongrass by one-pot synthesis (Brumbaugh et al., 2014). There was no absorption shown in the UV-Vis spectrum which may be attributed to the extremely small size of the NPs which were also devoid of SPR (Singh et al., 2010). Biogenic synthesis of CuNPs from *Citrus medica* juice was done showing a peak at 631 nm (Shende et al., 2015). The reduction was carried out in an aluminum vessel. The color of $CuSO_4$ changed to reddish brown after the addition of lemon juice which was followed by the deposition of shiny brown precipitate on the wall of the vessel which may be due to the displacement of the less reactive metal from a more reactive one (Eqs. 23.4-23.6; Sastry et al., 2013).

$$CuSO_4 + 2NaOH \rightarrow Cu(OH)_2 + Na_2SO_4 \quad (23.4)$$

$$CuSO_4 + 2NH_4OH \rightarrow Cu(OH)_2 + (NH_4)_2SO_4 \quad (23.5)$$

$$2Al_{(s)} + 3CuSO_{4(aq.)} \rightarrow 6Cu_{(s)} + Al_2(SO_4)_{3(aq.)} \quad (23.6)$$

23.5.1.5 Other metal nanoparticles

Mentha spicata leaf extract has been employed to synthesize crystalline FeNPs in the size range of 20−45 nm showing excellent As (III) and As (V) removal. Similarly, *S. jambos* and *Eichhornia crassipes* leaf extracts were employed to synthesize FeNPs (Xiao et al., 2016). Another green synthesis of FeNPs was reported from green tea extract (Kuang et al., 2013) and the NPs acted as Fenton-like catalysts to remove chemical oxygen demand from wastewater. MgNPs have been derived from *Hydrangea paniculata* flower extract having spherical and ellipsoidal structure (Ishak et al., 2019) and having appreciable antioxidant activity. Spherical polydisperse and crystalline SeNPs with a size range of 60−80 nm have been derived from the leaf extract of lemon leaf extract (Suranjit et al., 2013) and were utilized to prevent UV-induced DNA damage.

23.5.2 Metal-oxide nanoaprticles

Various applications of engineered metal oxide NPs have been proved. SiO_2 and TiO_2-based NPs have been found to enhance nitrate reductase activity in soybean and adsorption capacity for fertilizer along with the increased rate of photosynthesis (Hong et al., 2005). It is worth noting that nano-Al_2O_3 inhibits the root growth in maize and cucumbers (Yang and Watts, 2005). TiO_2 and AgNPs are naturally found and TiO_2 can generate reactive oxygen species (ROS) in the presence of UV light (Armelao et al., 2004). *Camellia sinensis* extract has been used to synthesize iron oxide NPs having irregular geometry, similarly, extracts of *A. indica*, *Hibiscus rosa-sinensis*, *Coriandrum sativum* and *Coriandum sinensis* have been employed to derive ZnONPs (Khusro et al., 2022). ZnO NPs have very large excitation energy (approximately 60 meV) and band-gap energy of 3.37 eV, making them suitable to be

used as semiconductors (Matinise et al., 2017). *Pongamia pinnata* leaves extract was used to synthesize ZnO NPs. The characterization revealed the spherical shape of the NPs with an average size of 100 nm (Rolim et al., 2019) and high purity. *Rubus coreanus* was used as a reducing agent for the synthesis of ZnO NPs and they were found to degrade Malachite Green dye (Ali et al., 2015). *Jatropha curcas* was used to synthesize TiO2 NPs and CuO NPs were derived from the extract of *Aloe barbadensis* and *Aloe sylvestris* (Jeevanandam, et al., 2016). Gum karaya has been employed to synthesize CuO NPs (Padil and Černík, 2013; Das et al., 2013). In the synthesis, a mixture of $CuCl_2$ and gum was heated at 75°C in an aqueous medium. CuO NPs are deposited on the surface of gum karaya due to their affinity for gum. CuO NPs from the leaf extract of Aloe vera have been reported to have a monoclinic structure with a particle size of 20 nm (Kumar et al., 2015). Cluster formation of CuO NPs was reported from *Ixoro coccinea* leaf extract (Vishveshvar et al., 2018) having an average size of 300 nm. Leguminous plants are abundant in proteins, flavonoids, alkaloids and amino acids and these phytoconstituents may act as reducing agents in the synthesis of metal NPs (Bachheti et al., 2019a,b). Monoclinic crystalline CuO NPs having an average size of 26.6 nm have been synthesized from the extract of black been (Nagajyothi et al., 2017). The proposed synthesis mechanism of CuO NPs involves the reaction of $CuSO_4$ with OH^- which is generated by the ionization of the water molecule and finally leads to the reduction of the phytoconstituents present in the seed extract. $CuSO_4$ remains ionized in an aqueous medium and may form $[Cu(H_2O)_6]$. Cu^{2+} ions get reduced by protein or polypohenol. Phenol in turn gets oxidized to a phenolate ion. The TiO2 NPs are easily reproducible and biosynthesis of TiO_2 NPs from different plants has been reported. The aqueous extract of *Eclipta prostrate* was used to synthesize TiO_2 NPs having a size range of 36−68 nm (Rajakumar et al., 2012). Similarly, the leaf extract of *Albizia saman* was employed to synthesize TiO_2 NPs at 50°C. (Subhashini and Nachiyar, 2014). The anatase form of TiO_2 NPs was obtained from the plant extract of *C. longa* (Jalill et al., 2016) having a size diameter of 160−220 nm. The herbal extract of *Echinacea purpurea* was employed for the synthesis of TiO_2 NPs having a size range of 120 nm (Dobrucka, 2017). The leaf extract of *Psidium guajava*is rich in alcohol and primary and aromatic amines which assisted in the formation of TiO_2 NPs. The physical, chemical and electronic properties of metal oxides and their potential for environmental remediation have encouraged researchers to further explore other metal oxide-based NPs. RuO_2NPs having an average size of 2.15 nm have been synthesized from *Aspalathus linearis* plant extract (Ismail et al., 2016). The NPs had an optical band gap of 2.1 eV with a high surface area. Another green synthesis was reported for the synthesis of Mn_3O_4NPs obtained from banana peel extracts (Yan et al., 2014). The ripe pomegranate seed extract was employed to obtain SnO_2NPs having good semiconductor properties (Kumari and Philip, 2015). *Citrus limon*, *Vitis vinifera* and *Cucumis sativus* extracts have been used to synthesize Fe_3O_4NPs for the removal of several antibiotics (Stan et al., 2017). Magnetic Fe_2O_3NPs from the fruit extract of *Cynometra ramiflora* have been reported to have spherical and rhombohedral structures (Sai Saraswathi et al., 2017), similarly spherical magnetite Fe_3O_4NPs from Andean blackberry leaves have been reported (Kumar et al., 2016) with enhanced photocatalytic dye degrading activity. A fast synthesis of hexagonal FeHCF nanostructures was produced from *S. mukorossi* which were found to be useful for the removal of organic pollutants from water and soil and converted poly aromatic hydrocarbons to nontoxic products (Shanker et al., 2017). Tables 23.1 and 23.2 discuss some of the recent studies associated with the plant-mediated

TABLE 23.1 Some of the recent studies on the plant-mediated synthesis of metal nanoparticles, synthesis conditions, their characterization, morphology, and applications.

Plant	Plant part used	Nanoparticle derived	Synthesis condition	Characterization techniques	Shape and size	Phytoconstituents	Application	Key reference
Phoenix dactylifera	Fruit	Pt	Solution-based; color change	FTIR, UV-Vis, XRD, SEM-EDX, TGA, TEM, HPLC	Spherical; 2.2–3 nm	Flavanoids and polyphenols	Anticancer and antibacterial	Al-Radadi (2019)
Cestrum nocturnum	Leaf	Ag	Extract mixed with ingredient; color change	UV-Vis, XRD, TEM, SEM, FTIR, EDS	Spherical; 20 nm	Alkaloids, flavanols, glycosides, steroidal saponins, and phenols	Antioxidant and antibacterial	Keshari et al. (2020)
Gelidium pusillium	Seaweed extract	Au	Reaction with content stirring at 60°C for 2 h	UV-Vis, FTIR, TEM, XRD, DLS	Spherical and pseudo-spherical; 7–17 nm	Proteins, lipids, and polyphenols	Anticancer	Jeyarani et al. (2020)
Hisbiscus sabdariffa	Flower	Au	Solution-based; mixing and stirring at room temperature for 30 mins; color change	FTIR, UV-Vis, XRD, FE-SEM, TEM	Spherical; 15–45 nm	Organic acids, flavanoids, polysaccharides, and polyphenols	Anti-acute myeloid leukemia, antioxidant, and anti-inflammatory	Zangeneh and Zangeneh (2020)
Nigella sativa	Seed	Pt	Mixing of ingredients; stirring at 75°C for 2 days	XRD, XPS, TEM, HRTEM, UV-Vis	Spherical; 1–6 nm	Alkaloids, terpenoids, saponins, and tannins	Amtimicrobial and anticancer	Aygun et al. (2020a,b)
Ganoderma lucidum	Mushroom	Ag	Mixing of ingredients; color change	XPS, XRD, TEM, UV-Vis, FTIR,	Spherical; 15–22 nm	Peptidoglycans, triterpenes, and polsaccharides	Antifungal	Aygun et al. (2020a,b)
Gossypium arboreum	Boll peel	Pd	Extract mixed with ingredient; reaction set at 60°C for 2 h	UV-Vis, SRP, XRD, TEM, FTIR	Spherical; 9.44 nm	Flavanoids, alkaloids, terpenoids, phenolic acids, and proteins	Catalytic activity against toxic azo-dyes	Narasaiah and Mandal (2020)

Pimenta dioica	Leaf	Au	Solution-based; mixing of ingredients; reaction set for completion	FTIR, UV-Vis, XRD, TEM, SERS, PASR	Spherical; 13 ± 4 nm	Polyphenols	Anticancer	Kharey et al. (2020)
Croton sparsiflorus	Leaf	Au	Extract mixed with ingredient; color change	FTIR, XRD, FE-SEM, TEM, UV-Vis	Spherical; 16.6–17 nm	Polyphenols and peptides	UV protection, antibacterial, and anticancer	Boomi et al. (2020)
Desmodium gangeticum	Leaf	Au	Mixing of ingredients; reaction set for completion	UV-Vis, FESEM, TEM, EDAX, XRD	Spherical; 16 ± 4 nm	Flavones and isoflavanoid glycosides	Antioxidant	Ghosh et al. (2020)
Litsea cubeba	Fruit	Au	Mixing of ingredients; vigorous stirring in dark; color change	FTIR, TEM, XRD, UV-Vis	Spherical; 8–18 nm	Alkaloids, terpenoids, flavanoids, steroids, lignans, and fatty acids	Catalytic reduction of 4-nitrophenol	Doan et al. (2020)
Elaeagnus umbellate	Fruit	Ag	Mixing; stirring for 30 mins	UV-Vis, FTIR, AFM, SEM	Spherical; 40 nm	Tetraterpenoids, flavanoids, and polyphenols	Antimicrobial	Ali et al. (2020)
Malus domestica	Fruit	Ag	Extract mixed with ingredient; kept in the water bath at 75°C	UV-Vis, TEM	Spherical; 16 nm	Polyphenols, anthocyanins, and flavanoids	Antimicrobial	Kazlagic et al. (2020)
Nauclea latifolia	Fruit	Ag	Ingredient mixed; incubated for 24–72 h	UV-Vis, XRD, EDX, SEM, FTIR	Irregular; 12 nm	Alkaloids, flavanoids, terpenoids, and anthoquiones	Antimicrobial and antioxidant	Odeniyi et al. (2020)
Orobanche aegyptiaca	Stem	Cu	Mixing of ingredients; stirred for 10–15 mins; kept in dark for 72 h	XRD, FTIR, SEM, EDX, TEM	Spherical; <50 nm	Polyphenols, tannins, alkaloids, and peptides	Nematicidal and antibacterial	Akhter et al. (2020)
Juglans regia	Shell	Cu	Extract mixed with ingredient; reaction set for completion	TEM, EDX, TGA, FTIR, XPS	Irregular; 15–22 nm	Lignin and cellulose	Antibacterial, antioxidant, and anticancer	Mehdizadeh et al. (2020)
Anacardium occidentale	Testa	Cu	Mixing and stirring at 60°–70°C for 15 mins; color change	FTIR, UV-Vis, SEM-EDS, XRD, HR-TEM	Irregular spherical; <20 nm	Flavanoids, polyphenols, and phenolic acids	Efficient removal of uranium	Chandra and Khan (2020)

(*Continued*)

TABLE 23.1 (Continued)

Plant	Plant part used	Nanoparticle derived	Synthesis condition	Characterization techniques	Shape and size	Phytoconstituents	Application	Key reference
Hagenia abyssinica	Leaf	Cu	Mixing of ingredients; color change	UV-Vis, UV-Drs, FTIR, XRD, SEM, EDXA, TEM, HR-TEM, SAED	Spherical, hexagonal, triangular and cylindrical; 34.76 nm	Polypheols, tannins, and glycosides	Antimicrobial	Murthy et al. (2020)
Syzygium aqueum	Leaf	Pd	Mixing of ingredients; reaction set in an oil bath at 90°C for 8 h	FTIR, BET, HR-TEM, ICP-Ms, TGA, XRD, FE-SEM/EDX	Irregular; 5–20 nm	Phenolic acids, alkaloids, flavanoids, polyols, and terpenoids	Catalysis in the coupling reaction	Manjare and Chaudhari (2020)
Rosamarinus officinalis	Leaf	Pd	Extract mixed with ingredient; reaction set for completion	FTIR, XRD, FE-SEM, TEM, UV-Vis	Semi-spherical; 15–90 nm	Flavanoids, alkaloids, and terpenoids	Catalysis, antibacterial, and antifungal	Rabiee et al. (2020)
Prosopis farcta	Fruit	Pt	Solution-based; sonochemical method	XRD, FESEM, TEM, EDX	Irregular; 3.5 nm	Alkaloids, flavanoids, and tannins	Antimicrobial and anticancer	Jameel et al. (2020)
Tragia involucrate	Leaf	Pt	Solution-based; stirring at 50°C for 1 h	FTIR, XRD, SPR, SEM	Spherical; 10 nm	Polyphenols, alkaloids, flavanoids, and proteins	Biomedical and pharmaceutical	Selvi et al. (2020)
Oreganum vulgare	Leaf	Ag	Mixing of ingredients; reaction at room temperature for 2 h	FTIR, UV-Vis, TEM, EDS, XRD	Spherical; 136 nm	Polyphenols	Antibacterial and antioxidant	Salayová et al. (2021)
Dalbergia ecastophyllum	Plant extract	Au	Mixing of ingredients; reaction set at particular pH and optimized temperature for 1 h	FTIR, HR-TEM, EDXS, TGA, SAED	Spherical; 8–15 nm	Flavanoids, isoflavanoids, and terpenoids	Antibacterial, antifungal, and anticancer	Botteon et al. (2021)
Persicaria salicifolia	Leaf	Au	Extract mixed with ingredient; color change	UV-Vis, EDX-SEM, FTIR, HRTEM, XRD, SAED, XPS, EDX, XPS	Spherical; 5–23 nm	Glycosides, flavanoids, and polyphenols	Antioxidant and anticancer	Hosny and Fawzy (2021)

Lilium candidum	Flower	Pt	Mixing of ingredients; incubated at 70°C for 12 h	UV-Vis, XRD, FTIR, TEM	1.42 ± 0.33 nm	Polysaccharides	Catalysis and detection of glucose and glutathione	Fan et al. (2021)
Phragmites australis	Leaf	Au	Solution-based; color change	HRTEM, UV-Vis, XRD, FTIR, EDX, XPS, zeta potential	Spherical; 18 nm	Glycosides, tannins, flavanoids, terpenoids, and phenolic compounds	Anticancer, antioxidant, and photocatalysis	El-Borady et al. (2021)
Salix tetrasperma	leaf	Pt	Extract mixed with ingredient; sonication	XRD, FTIR, UV, TEM, SEM, EDX	Spherical; 17.84 nm	Flavanoids, saponins, terpenoids, and phenolic glycosides	Anticancer, antioxidant, and photocatalytic	Ramachandiran et al. (2021)
Ricinus communis	Seed	NZVI	Mixing of ingredients; reaction set for completion	TEM, SEM, FTIR, EDS, XRD, XPS, zeta potential	Spherical; 20 nm	Flavanoids, terpenoinds, organic and phenolic acids, and proteins	Removal of methylene blue from water	Abdelfatah et al. (2021)
Vaccinium myrtillus	Fruit	Cu	Mixing of ingredients; incubated at 50°C for 2 h	VIS, XPS, HPLC-Ms, TEM	9.91 nm	Anthocyanins	Antimicrobial	Benassai et al. (2021)
Atriplex halimus	Leaf	Pt	Mixing and stirring at 95°C for 1 h; reaction set at particular pH; color change	FTIR, UV-Vis, EDX, XRD, HRTEM, SAED, XPS	Spherical; 1–3 nm	Flavanoids, glycosides, and alkaloids	Catalytic, antibacterial, and antioxidant	Eltaweil et al. (2022)
Polygonum salicifolium	Leaf	Pt	Extract mixed with ingredient; color change	FTIR, UV-Vis, XRD, HRTEM, EDX, SAED, XPS, zeta potential	Spherical; 1–3 nm	Polyphenols	Antimicrobial, antidiabetic, antioxidant, and catalytic	Hosny et al. (2022)
Cordyceps militaris	Flower	Pt	Extract mixed with ingredient; stirred at 50°C for 1 h	UV-Vis, DLS, FE-SEM, EDS, TEM, XRD, FTIR	13.34 ± 4.06 nm	Proteins and polysachharides	Antioxidant and antibacterial	Liu et al. (2022)

(*Continued*)

TABLE 23.1 (Continued)

Plant	Plant part used	Nanoparticle derived	Synthesis condition	Characterization techniques	Shape and size	Phytoconstituents	Application	Key reference
Allium fistulosum	Leaf	Pd	Solution-based; color change	FTIR, UV-Vis, XRD, SEM, TEM	Spherical; 500 nm	Flavanoids and terpenoids	Antibacterial, antifungal, antioxidant, and antidiabetic	Vinodhini et al. (2022)
Physalis minima	Plant extract	Au	Mixing of ingredients; stored in the dark	UV-Vis, XRD, FTIR, zeta potential	Spherical; 36 nm	Flavanoids, phenols, and polyphenols	Antioxidant, antibacterial, and antidiabetic	Sekar et al. (2022)
Hypericum perforatum	Leaf, stem	Ag	Extract mixed with ingredient; reaction set at 80°C for 4 h	UV-Vis, ATR-IR, XRD, TGA, zeta potential	Spherical; 20−40 nm	Anthoquinones and flavanoids	Antibacterial	Alahmad et al. (2022)
Origanum majorana	Leaf	Ag	Reaction set at 70°C for 1 h; color change	UV-Vis, TEM, FTIR, EDX, XRD	Spherical; 26.63 nm	Phenolic compounds	Antibacterial	Yassin et al. (2022)

TABLE 23.2 Some of the recent studies on the plant-mediated synthesis of metal-oxide nanoparticles, synthesis conditions, their characterization, morphology, and applications.

Plant	Plant part used	Nanoparticle derived	Synthesis condition	Characterization techniques	Shape and size	Phytoconstituents	Application	Key reference
Acalypha fruticosa	Leaf	ZnO	Solution-based; reaction set for completion	UV-VIS, FTIR, HR-SEM, TEM, EDAX, AFM	Spherical and hexagonal; 50 nm	Flavanoids	Antimicrobial	Vijayakumar et al. (2020)
Prosopis juliflora	Leaf	ZnO	Extract mixed with ingredient; reaction at 170°C for 5 h	FTIR, XRD, UV-Drs, FE-SEM, HR-TEM,EDAX,	Irregular; 31.80−32.39 nm	Flavanoids, polyphenols, and alkaloids	Antibacterial and degradation of methylene blue	Sheik Mydeen et al. (2020)
Calotropis gigantean	Leaf	ZnO	Solution based; combustion method	FTIR, UV-Drs, XRD, SEM, EDAX, HR-TEM, SAED	Hexagonal and pyramidal; 10−50 nm	Alkaloids and flavanoids	Nitrite sensing, photocatalysis, and antibacterial	Kumar et al. (2020)
Urtica dioica	Leaf	ZnO	Solution-based; color change	FTIR, UV-Vis, GC-Ms, XRD, SEM, TEM, EDX, TGA	Spherical; 20−22 nm	Polyphenols	Antidiabetic	Bayrami et al. (2020)
Citrus lemon	Lemon peel	TiO_2	Mixing of ingredients; reaction at room temperature for 5 h; color change	UV-Vis, XRD, EDX, SEM, TEM	Spherical; 80−140 nm	Alkaloids, oraganic acids, and flavanoids	Photocatalysis	Nabi et al. (2022)
Menthe arvensis	Leaf	TiO_2	Extract mixed with ingredient; reaction at 50°C for 5 h	FTIR, UV-Vis, XRD, FESEM	Spherical; 20−70 nm	Alkaloids, phenols, and terpenoids	Antimicrobial	Ahmad et al. (2020a,b,c)
Euphorbia herita	Leaf	Fe_2O_4	Stirring for 3 h; reaction set at particular pH; color change	UV-Vis, FTIR, SEM, XRD	25−80 nm	Polyphenols, flavanoids, and alcoholic compounds	Antibacterial and antifungal	Ahmad et al. (2020a,b,c)
Kniphofia foliosa	Root	TiO_2	Extract mixed with ingredient; stirred for 4 h	TGA/DTA, ZRD, SEM-EDS, TEM, UV-Vis, FTIR	Spherical; 10.2 nm	Anthraquinone	Antibacterial	Bekele et al. (2020)

(*Continued*)

TABLE 23.2 (Continued)

Plant	Plant part used	Nanoparticle derived	Synthesis condition	Characterization techniques	Shape and size	Phytoconstituents	Application	Key reference
Phoenix dactylifera	Pulp	ZnO	Extract mixed with ingredients; reaction set for completion	EDX, XPS, UV-Vis, FTIR, XRD, DSC/TGA, SEM, TEM photoluminescence	Spherical; 29.3 nm	Flavanoids, quinines, caretenoids, sterols, and anthocyanins	Dye degradation and antibacterial	Rambabu et al. (2021)
Chromolaena odorata	Leaf	SnO_2	Extract mixed with ingredient; stirred at ambient temperature for 3 h	XRD, FTIR, FESEM, EDX, UV-Vis	Spherical; 28 nm	Flavanoids	Catalysis and optoelectronic appliances	Buniyamin et al. (2022)
Bougainvillea glabra	Flower	CuO	Mixing of ingredients; color change	FTIR, TEM, XRD, UV-Vis	Spherical; 12 ± 4 nm	Amides and aromatic groups	Antifungal	Shammout et al. (2021)
Psidium guajava	Leaf	CuO	Mixing of ingredients; color change	UV, FTIR, XRD, FESEM, SAED, EDS, DLS	40–150 nm	Polyphenols ad flavanoids	Biomedical	Sathiyavimal et al. (2021)
Cissus vitiginea	Leaf	CuO	Extract mixed with ingredients; color change	XRD, TEM, EDS-SEM	Spherical; 32.32 nm	Polyphenols, anthoquinones, flavanoids, terpenoids, anthrones, and reducing sugars	Antioxidant	Thakar et al. (2022)
Thymbra spicata	Leaf	ZnO	Mixing of ingredients; reaction set for completion	FTIR, XRD, UV-Vis, EDX, SEM	Spherical; 6.5–7.5 nm	Polyphenols and flavanoids	Antimicrobial, antioxidant, and protecting cells against DNA damage	Gur et al. (2022)
Calotropis procera	Plant extract	CuO	Mixing of ingredients; reaction set for completion	FTIR, UV-Vis, XRD, SEM, TEM	Spherical; 20–80 nm	Polyphenols	Antibacterial, antifungal, and antioxidant	Shah et al. (2022)

Canthium coromandelicum	Leaf	CuO	Mixing of ingredients; color change	FTIR, FESEM, HR-TEM, XRD, UV-Vis	Spherical; 33 nm	Phenols, saponins, and alkaloids	Degradation of organic dyes	Selvam et al. (2022)
Hibiscus rosa sinensis	Flower	Fe_2O_3	Extract mixed with ingredients; reaction set for completion	UV-Vis, FTIR, XRD, TEM	Spherical; 51 nm	Polyphenols and alkaloids	Antibacterial	Buarki et al. (2022)
Acorus calamus	Leaf	TiO_2	Mixing of ingredients; reaction set for completion	UV, FTIR, SEM, DLS, BET, TGA-DSC, XRD	Globular; 15−40 nm	Flavanoids, terpenes, quinines, and phenylpropanoids	Antimicrobial	Ansari et al. (2022)
Phyllanthus niruri	Leaf	Fe_2O_3	Ultrasonication	FTIR, XRD, XPS, BET, HR-TEM, EDX	Spherical; 19.3 nm	Phyllathi, flavaoids, tannins, glycosinoids, and hypophyllanthin	Photocatalytic, degradation of organic dyes	Haseena et al. (2021)
Camellia senensis	Leaf	MgO	Extract mixed with ingredient; color change	XRD, SEM, FTIR, UV-Vis, DSC, TGA	Spherical; 65 ± 5 nm	Flavanoids and catechin	Photocatalytic degradation of organic dyes	Kumar et al. (2022)

synthesis of metal and metal-oxide NPs, characterization techniques employed and their application.

23.6 Characterization of nanoparticles

The characterization is used to explore the various enhanced properties of nanomaterials that are different from bulk materials. There were advanced sophisticated instruments were used to address the issue of characterization of nanostructures viz, XRD has been used for determining crystalline character, crystal size, structure and lattice constant of NPs while SEM & TEM is generally used for morphological characterization of NPs. The chemical composition, purity and stability are checked by FTIR, UV-VIS spectroscopy, Energy dispersive X-ray spectroscopy (EDX) and Zeta potential (Rahman et al., 2013a,b; Modena et al., 2019; Husen, 2020).

23.6.1 UV-VIS absorption spectroscopy

UV-Visible spectroscopy is often used to study the behavior of light absorbed and scattered by sample nanomaterials. The SPR band in metallic NPs and absorption spectra for semiconductor nanomaterials show different colors as their size is varied which is illustrated in Table 23.3 (Bhagyaraj and Oluwafemi, 2018).

Interestingly, the plasmonic NPs like gold and silver as well as metal oxide *viz* zinc oxide have optical properties that are very sensitive to size, shape, and concentration, which makes UV-VIS spectroscopy a valuable tool for monitoring the progress of the reaction and studying the effect different parameter for fabrication of NPs (Husen et al., 2019; Mishra et al., 2019). Recently, Hosny et al. (2022a,b) reported a simple biogenic route to synthesize gold NPs using *Tecoma capensis* leaf extract; as the leaf extract was added to gold ion solution, there was an immediate color change observed which confirmed the progress of the reaction. A distinct SPR peak at 515 nm signified the formation of gold NPs as shown in Fig. 23.2(A). Additionally, the synthesized gold NPs remain stable for up to three months (Fig. 23.2A) there was almost no change in SPR peak intensity as well position. In similar, Alahmad et al. (2021) successfully reported the fabrication of silver

TABLE 23.3 Relations between size and color of nanoparticles.

Nanoparticle	Size and shape	Color
Gold	10–20 nm	Red
	2–5 nm	Yellow
	>20 nm	Purple
Silver	40 nm	Blue
	100 nm	Yellow
	Prism shape Red	Prism shape Red

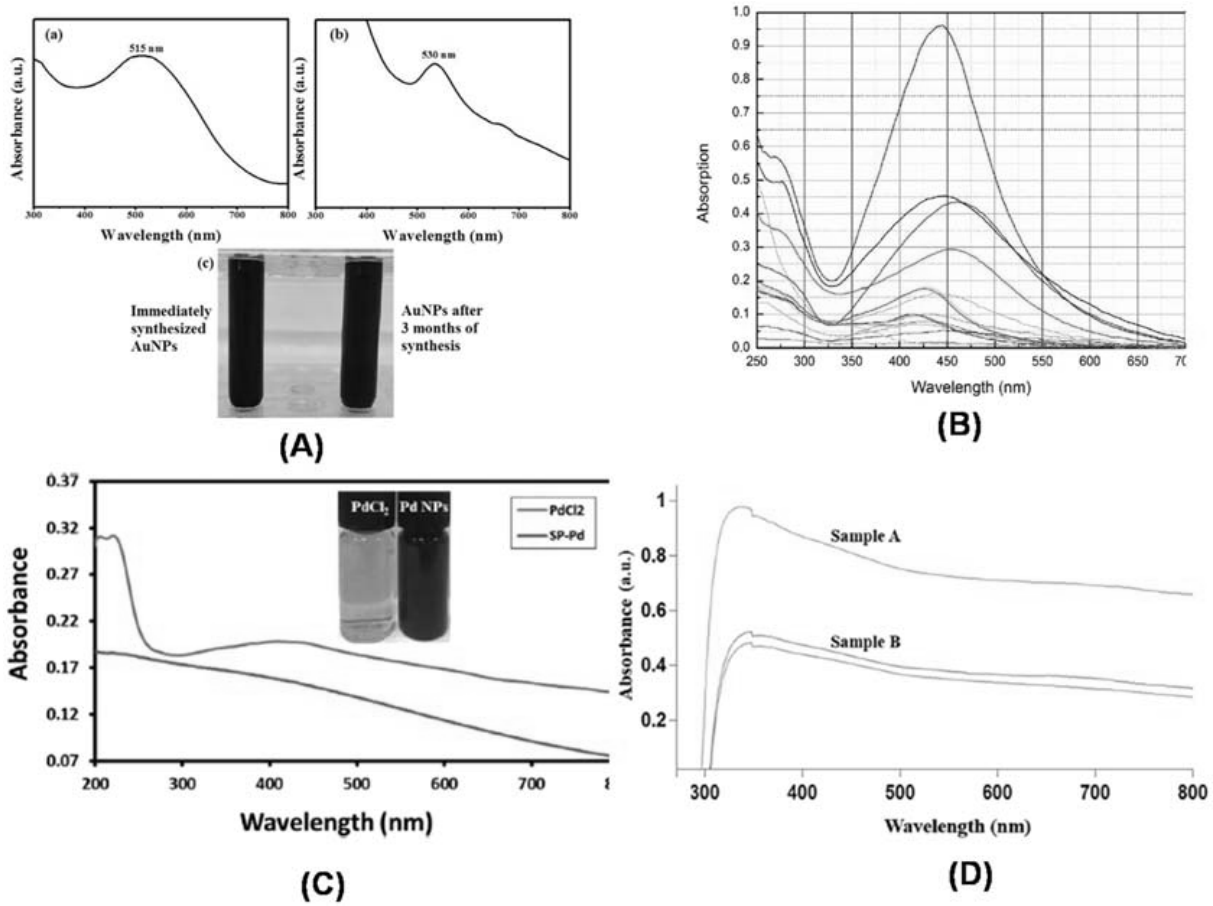

FIGURE 23.2 (A) Typical UV−Vis absorption spectrum of AuNPs using *Tecoma capensis* leaf extract (a) immediately (b) after 3 months (c) Image reveals the color change for gold NPs with time (B) UV-Vis spectra of AgNPs reveal the effect of varying the concentration of $AgNO_3$ with plant *Hypericum perforatum* L. extract (C) UV-Vis spectra of the corresponding solution depicting the reduction of PdCl2 to metallic Pd (D) UV-VIS spectra of ZnO NPs at two different plant extract concentrations. *Source: (A) Adopted from Hosny, M., Fawzy, M., El-Badry, Y.A., Hussein, E.E., Eltaweil, A.S., 2022a. Plant-assisted synthesis of gold nanoparticles for photocatalytic, anticancer, and antioxidant applications. J. Saudi Chem. Soc. 26, 101419. https://doi.org/10.1016/j.jscs.2022.101419; Hosny, M., Fawzy, M., El-Fakharany, E.M., Omer, A.M., El-Monaem, E.M.A., Khalifa, R.E., et al., 2022b. Biogenic synthesis, characterization, antimicrobial, antioxidant, antidiabetic, and catalytic applications of platinum nanoparticles synthesized from Polygonum salicifolium leaves. J. Environ. Chem. Eng. 10, 106806. https://doi.org/10.1016/j.jece.2021.106806. (B) Adopted from Alahmad, A., Feldhoff, A., Bigall, N.C., Rusch, P., Scheper, T., Walter, J.-G., 2021. Hypericum perforatum L.-mediated green synthesis of silver nanoparticles exhibiting antioxidant and anticancer activities. Nanomaterials 11, 487. https://doi.org/10.3390/nano11020487. (C) Adopted from Khan, Mujeeb, Albalawi, G.H., Shaik, M.R., Khan, Merajuddin, Adil, S.F., Kuniyil, M., et al., 2017. Miswak mediated green synthesized palladium nanoparticles as effective catalysts for the Suzuki coupling reactions in aqueous media. J. Saudi Chem. Soc. 21, 450−457. https://doi.org/10.1016/j.jscs.2016.03.008. (D) Adopted from Jayachandran, A., Aswathy, T.R., Nair, A.S., 2021. Green synthesis and characterization of zinc oxide nanoparticles using Cayratia pedata leaf extract. Biochem. Biophys. Rep. 26, 100995. https://doi.org/10.1016/j.bbrep.2021.100995.*

NPs using *H. perforatum* L. extract. Unsurprisingly, the bioreduction of silver ions was visually clear from color change as the aqueous extract was gradually mixed with silver ions, the color changed from pale light to yellowish brown and finally, the reddish-brown

color appeared, which attributes to the formation of silver NPs. He also studied the effect of varying parameters on the fabrication of silver NPs viz. observed change in color of the solution according to the concentration of silver NPs in solution as depicted in Fig. 23.2(B). The broadening of peaks for some samples attributes silver NPs to be aggregated or polydisperse. Khan et al. (2017) wield root extract of *Salvadora persica* L (Miswak) as a reducing agent for facile synthesis of PdNPs. With the gradual mixing of root extract with an aqueous solution of $PdCl_2$ under continuous stirring at 90°C for 2 hours, there was a change in color of the $PdCl_2$ solution from light brown to dark brown as depicted in Fig. 23.2(C). The Pd^{2+} ions showed a characteristic UV-Vis absorption band at 415 nm as the reaction was accomplished this band disappeared which attributes to the bioreduction of Pd^{2+} ions and confirmed the formation of Pd^0 NPs. Jayachandran et al. (2021) reported an eco-friendly simple route to fabricate zinc oxide NPs using different plant extract concentrations of *Cayratia pedata* and the reaction temperature was maintained at 55°C, 65°C, and 75°C. The presence of secondary metabolites in *Cayratia pedata* extract was acting as a reducing as well as capping agent for the biofabrication of zinc oxide NPs which was confirmed by UV-Vis absorption spectrum as depicted in Fig. 23.2(D) a peak at 320 nm attribute the formation of zinc oxide NPs. Interestingly, Fig. 23.2D shows the UV-VIS absorption spectrum of zinc oxide at two different plant extract concentrations. Sample A shows more absorption in comparison to sample B, owing to a higher concentration of plant extract (Hosny et al., 2022a,b; Alahmad et al., 2021; Khan et al., 2017).

23.6.2 Fourier transform infrared spectroscopy

It is an important analytical tool that is widely used to elucidate the structure of individual molecules as well as organic mixtures. FTIR spectroscopy uses modulated mid-infrared energy to interrogate a sample. Upon illumination of the photon on the molecule, it creates undulating motion at specific frequencies and attributes to the strength of the bond between atoms in molecules. When the energy of undulating motion and bond energy becomes equal, absorption occurs as there are different bonds present in the molecules, and hence there are different absorptions of IR radiation (Skoog et al., 1988). Generally, organic compounds contain carbon, hydrogen, nitrogen, oxygen, halogens, phosphorus, silicon, and sulfur hence they absorb infrared radiation and are easily characterized by FTIR. In the last few years, the biogenic synthesis of NPs by secondary metabolites present in the plants has received great attention because it provides an easy cost-effective method against the conventional mode of synthesis. Recently, Hosny et al. (2022a,b) fabricate gold NPs using *T. capensis* extract and successfully reported that there were several peaks in the FTIR spectrum of neat extract as shown in Fig. 23.3(A) which belongs to different functional groups viz. H-bonded O−H at 3200/cm that shifted to higher wavenumber (3278/cm) in the spectrum of *T. capensis* assisted synthesis of AuNPs with lower intensity. The FTIR spectrum confirmed that the plant extracts rich in secondary metabolites viz. alkaloids, flavonoids, glycosides, terpenoids, and tannins were responsible for the bio-reduction of Au^+ ions into AuNPs and acted as stabilizing and capping agents as well. Similarly, Sharifi-Rad et al. (2020) employed an eco-friendly and cost-effective method to synthesize AgNPs using *A. tribuloides* Delile root extract. Interestingly,

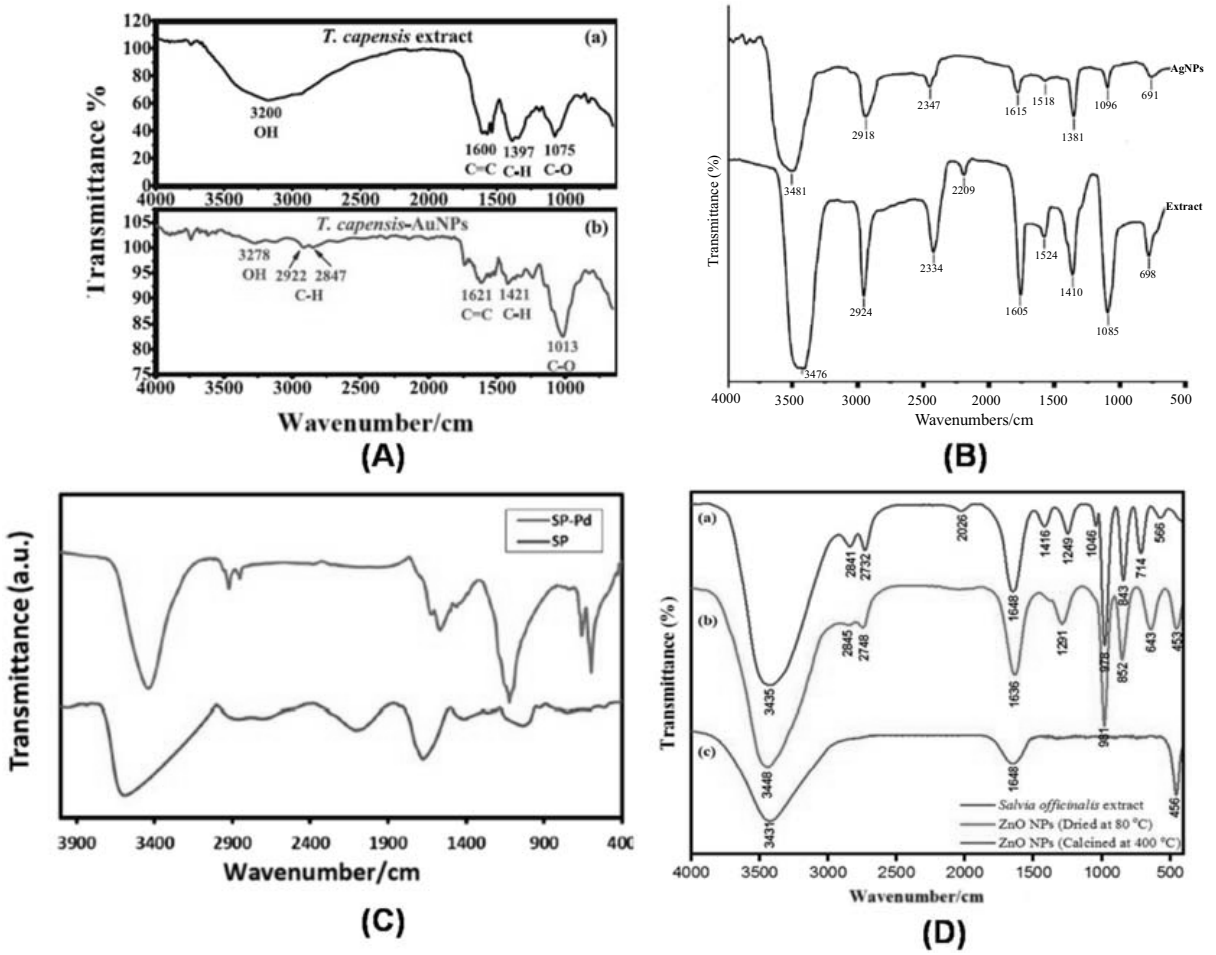

FIGURE 23.3 Typical Fourier transform-infrared spectra (A) FTIR of (a) *Tecoma capensis* extract (b) *T. capensis*-AuNPs (B) FT-IR of the A. tribuloides root extract and the greenly synthesized AgNPs (C) FT-IR of pure green-synthesized palladium nanoparticles (PdNPs) (*blue* line) and *Salvadora persica L.* root extract (*red* line) (D) FTIR of aqueous leaf extract of *Salvia officinalis* and greenly synthesized ZnO NPs dried at 80°C &calcinated at 400°C. *Source: (A) Adopted from Hosny, M., Fawzy, M., El-Badry, Y.A., Hussein, E.E., Eltaweil, A.S., 2022a. Plant-assisted synthesis of gold nanoparticles for photocatalytic, anticancer, and antioxidant applications. J. Saudi Chem. Soc. 26, 101419. https://doi.org/10.1016/j.jscs.2022.101419; Hosny, M., Fawzy, M., El-Fakharany, E.M., Omer, A.M., El-Monaem, E.M.A., Khalifa, R.E., et al., 2022b. Biogenic synthesis, characterization, antimicrobial, antioxidant, antidiabetic, and catalytic applications of platinum nanoparticles synthesized from Polygonum salicifolium leaves. J. Environ. Chem. Eng. 10, 106806. https://doi.org/10.1016/j.jece.2021.106806. (B) Adopted from Sharifi-Rad, M., Pohl, P., Epifano, F., Álvarez-Suarez, J.M., 2020. Green synthesis of silver nanoparticles using Astragalus tribuloides delile. root extract: characterization, antioxidant, antibacterial, and anti-inflammatory activities. Nanomaterials 10, 2383. https://doi.org/10.3390/nano10122383. (C) Adopted from Khan, Mujeeb, Albalawi, G.H., Shaik, M.R., Khan, Merajuddin, Adil, S.F., Kuniyil, M., et al., 2017. Miswak mediated green synthesized palladium nanoparticles as effective catalysts for the Suzuki coupling reactions in aqueous media. J. Saudi Chem. Soc. 21, 450–457. https://doi.org/10.1016/j.jscs.2016.03.008. (D)Adopted from Abomuti, M.A., Danish, E.Y., Firoz, A., Hasan, N., Malik, M.A., 2021. Green synthesis of zinc oxide nanoparticles using salvia officinalis leaf extract and their photocatalytic and antifungal activities. Biology 10, 1075. https://doi.org/10.3390/biology10111075.*

the FTIR spectrum of the extract revealed [Fig. 23.3(B)] that the absorption peak at 3476/cm corresponded to O-H stretching vibrations in alcohols and phenolic compounds while a distinct peak at 2924/cm related to the C-H stretching vibrations in the CH_3 group and apart from that there were clear and distinguished peaks at 2334, 2209, 1605 and 1514/cm for different functional groups which were presents in the plant extract. It was observed that there was a significant shifting of these peak positions as well as their intensity which confirmed that during the synthesis of AgNPs it not only worked as a reducing agent but also capped the AgNPs. It also prevented the agglomeration of AgNPs and enhancedtheir stability. Fig. 23.2(C) represents the FTIR spectrum for pure green synthesized palladium NPs and *Salvadora persica* L. root extract it has been observed that most absorption peaks reappear in the FTIR spectrum of Pd NPs with a slightly shifting peak position. The presence of absorption peaks at 3488, 2960, 1626, and 1156/cm in the FTIR of PdNPs strongly suggest that the phytomolecules of *Salvadora persica* were not only acting as reducing agents but it could also act as capping ligands on the surface of the PdNPs (Khan et al., 2017). Recently, Abomuti et al. (2021) have successfully explored the role of *Salvia officinalis* plant extract in the fabrication of ZnO NPs without using any other additive. Fig. 23.2(D) depicts the FTIR spectra of leaf extract showing distinct peaks at 891/cm for 1 & 2 degrees N-H groups, peaks at 1089 and 1026/cm represented stretching vibrations for -N-H, -C-O, and = C-H for various aliphatic amine, phenol, and carboxylic acid groups, while a peak at 1290/cm was attributed to the stretching of C-N and N-H bonds of aromatic amine phytochemicals and a broad peak at 3445/cm, reflected the presence of N-H and -O-H groups. These secondary metabolites may play a pivotal role in the biological synthesis of zinc oxide NPs by acting as a stabilizing agent as well as a capping agent. Unlikely, it has been observed that after multiple washes of zinc oxide NPs with water and ethanol and dried at 80°C, still there was the presence of biological moieties of plant extract on the surface of ZnO (Fig. 23.3D) which disappeared in the FTIR spectrum as the sample was calcined at 400°C. But the presence of peaks at 453 and 456/cm was attributed to the Zn-O stretching vibration and confirmed the formation of ZnONPs (Hosny et al., 2022a,b; Sharifi-Rad et al., 2020; Khan et al., 2017).

23.6.3 Transmission electron microscopy

TEM is a very powerful tool to elucidate the microstructural, crystal structure as well morphological information with high spatial resolution. Generally, it is used to study particle size, grain size, and distribution of particles in materials (Murty et al., 2013). In TEM analysis, an electron beam possessing a very high kinetic energy of about 100 keV is allowed to pass through a thin specimen (less than 200 nm) and obscure the important features of the sample which could not be studied by other characterization methods. Apart from morphological characterization, TEM offered special resolution down to an angstrom high magnification up to 10^6 & hence it can work as a microscope as well as a diffractometer. For the facile synthesis of nanomaterials, the TEM analysis played a very pivotal role in the morphological, crystallographic as well compositional study. Fig. 23.4A unveils the well-defined high-resolution transmission electron microscope (HRTEM) images of AuNPs synthesized using *T. capensis* extract. Interestingly it was observed that most of the

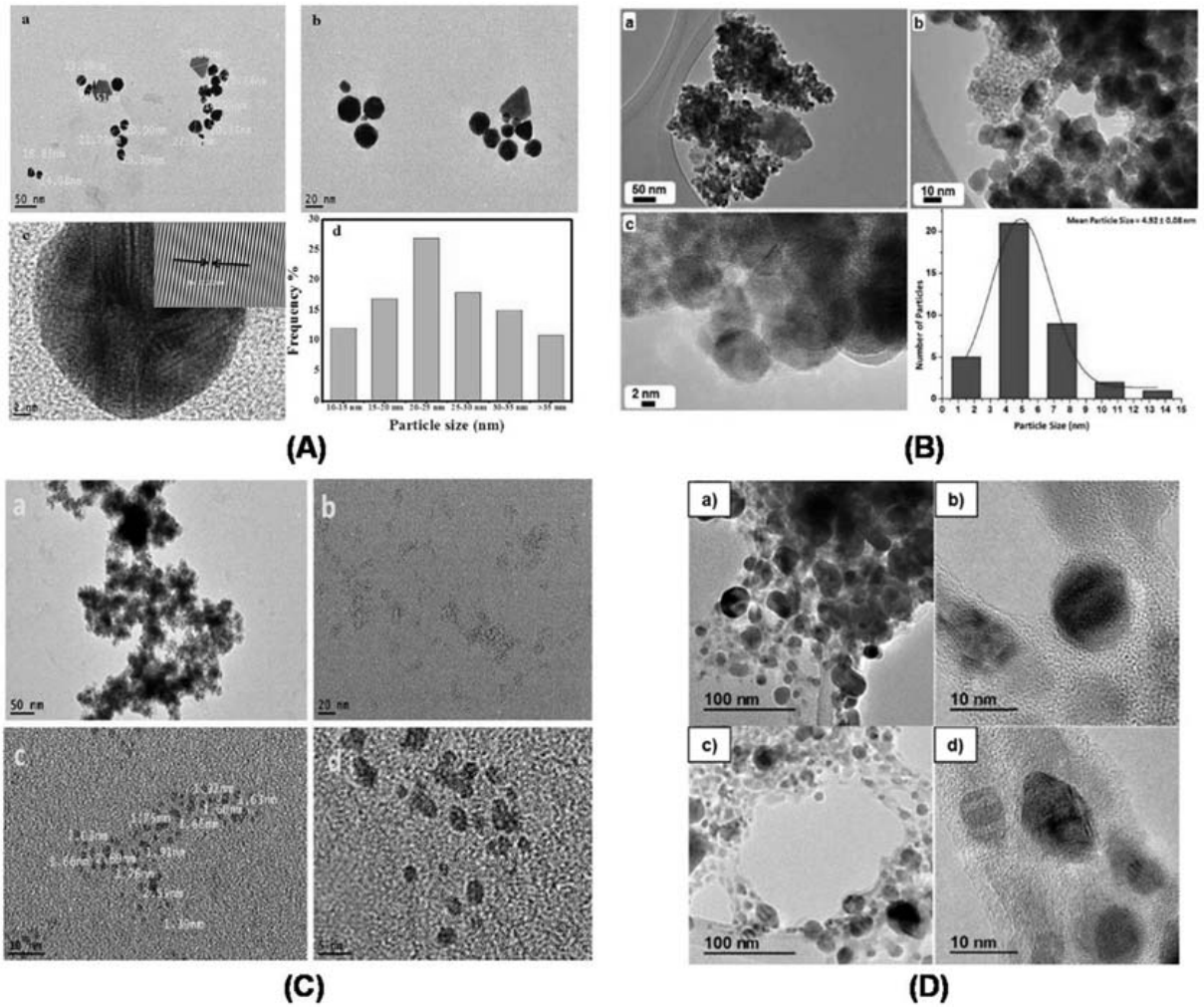

FIGURE 23.4 (A) High-resolution Transmission electron microscope (HRTEM) images (a–c) of *Tecoma capensis*-AuNPs (d) Particle size distribution histogram (B) TEM & HRTEM images of the PdNPs (a) overview, (b) and (c)magnified HRTEM image (d) particle size distribution graph (C) HRTEM images of PtNPs synthesized using *Atriplex halimus* leave (D) TEM micrographs of silver NPs obtained by green synthesis from safflower waste aqueous extract. *Source: (A) Adopted from Hosny, M., Fawzy, M., El-Badry, Y.A., Hussein, E.E., Eltaweil, A.S., 2022a. Plant-assisted synthesis of gold nanoparticles for photocatalytic, anticancer, and antioxidant applications. J. Saudi Chem. Soc. 26, 101419. https://doi.org/10.1016/j.jscs.2022.101419; Hosny, M., Fawzy, M., El-Fakharany, E.M., Omer, A.M., El-Monaem, E.M.A., Khalifa, R.E., et al., 2022b. Biogenic synthesis, characterization, antimicrobial, antioxidant, antidiabetic, and catalytic applications of platinum nanoparticles synthesized from Polygonum salicifolium leaves. J. Environ. Chem. Eng. 10, 106806. https://doi.org/10.1016/j.jece.2021.106806. (B) Adopted from Khan, M., Albalawi, G.H., Shaik, M.R., Khan, M., Adil, S.F., Kuniyil, M., et al., 2017. Miswak mediated green synthesized palladium nanoparticles as effective catalysts for the Suzuki coupling reactions in aqueous media. J. Saudi Chem. Soc. 21, 450–457. https://doi.org/10.1016/j.jscs.2016.03. (C) Adopted from Eltaweil, A.S., Fawzy, M., Hosny, M., Abd El-Monaem, E.M., Tamer, T.M., Omer, A.M., 2022. Green synthesis of platinum nanoparticles using Atriplex halimus leaves for potential antimicrobial, antioxidant, and catalytic applications. Arab. J. Chem. 15, 103517. https://doi.org/10.1016/j.arabjc.2021.103517. (D) Adopted from Rodríguez-Félix, F., López-Cota, A.G., Moreno-Vásquez, M.J., Graciano-Verdugo, A.Z., Quintero-Reyes, I.E., Del-Toro-Sánchez, C.L., et al., 2021. Sustainable-green synthesis of silver nanoparticles using safflower (Carthamus tinctorius L.) waste extract and its antibacterial activity. Heliyon 7, e06923. https://doi.org/10.1016/j.heliyon.2021.e06923.*

particles were spherical and had average particle sizes between 10 and 35 nm as displayed in a histogram. Additionally, other shapes were also detected viz. triangle, rhomboid, hexagonal, and irregular (Hosny et al., 2022a,b). Similarly, Fig. 23.4B displays clear HRTEM images of PdNPs synthesized via. the green route. It was observed that synthesized PdNPs were spherical with an average particle size diameter of about 10−20 nm. The high-resolution images revealed that synthesized PdNPs were highly crystalline with a narrow size distribution, which was attributed to the secondary metabolites present in *Salvadora persica* and worked as stabilizing agents. This was confirmed through the FTIR spectrum of Pd NPs as well as a close investigation of TEM images of PdNPs which supported the presence of light organic layers on the PdNPs (Khan et al., 2017). Fig. 23.4C represents the high-resolution images of PtNPs which revealed the homogenous distribution of PtNPs with an average particle size between 1 and 3 nm. Furthermore, hydrodynamic size was measured via. zetasizer, and it was found to be 10 nm as shown in Fig. 23.4B which was attributed to the presence of biomolecules on the surface of PtNPs (Dong et al., 2021; Ullah et al., 2017). Moreover, Selected Area Electron Diffraction (SAED) results confirmed the synthesized NPs possess high crystallinity and particles grown along the (111), (200), (220), and (311) planes and the results were inconsistent with XRD analysis. Fig. 23.4(D) displayed high magnified images of AgNPs fabricated using aqueous extract of safflower waste. The micrograph confirmed the fabricated AgNPs were almost spherical while other shapes were also detected as oval and irregular. The average particle diameter and particle size distribution were calculated from a high-resolution micrograph of TEM. Interestingly, it was found that AgNPs showed a range of particle size between 3 and 30 nm however 65% of particles are between 5 and 10 nm, which is interesting. Moreover, SAED studies confirmed the synthesized AgNPs were highly crystalline and clear circular points and diffraction rings at (111), (200), (220) and (311) planes attributable to the cubic planes of silver (Rodríguez-Felix et al., 2021).

23.6.4 Other important characterization techniques

There are different analytical techniques used to determine the physical, chemical, microstructural & mechanical properties of materials viz XRD, X-Ray Photoelectron Spectroscopy (XPS), Energy-dispersive X-ray spectroscopy (EDX), Zeta potential analyzer, etc. As the biogenic synthesis of NPs is always facilitated by secondary metabolites which are responsible for the bioreduction of metal ions and hence; zeta potential plays a very active tool to determine the net surface charge change on the synthesized NPs as well as its stability. Fig. 23.4A & B displayed characteristic zeta potential graphs of Au & Pt NPs respectively. Generally, the NPs possess the zeta potential value of more than +25 mV or less than −25 mV, showing excellent stability as well as a high degree of electrostatic repulsion (Murty et al., 2013). As the AuNPs were synthesized using *T. capensis* extract, the zeta potential value was about −24.5 mV (Fig. 23.5A) which confirmed the high stability of AuNPs. Similarly; it was found that the value of zeta potential for green synthesized PtNPs was about −25.4 mV (Fig. 23.4B), confirming their high stability. Typically, XRD provides information about the crystalline structure, lattice parameters as well as particle

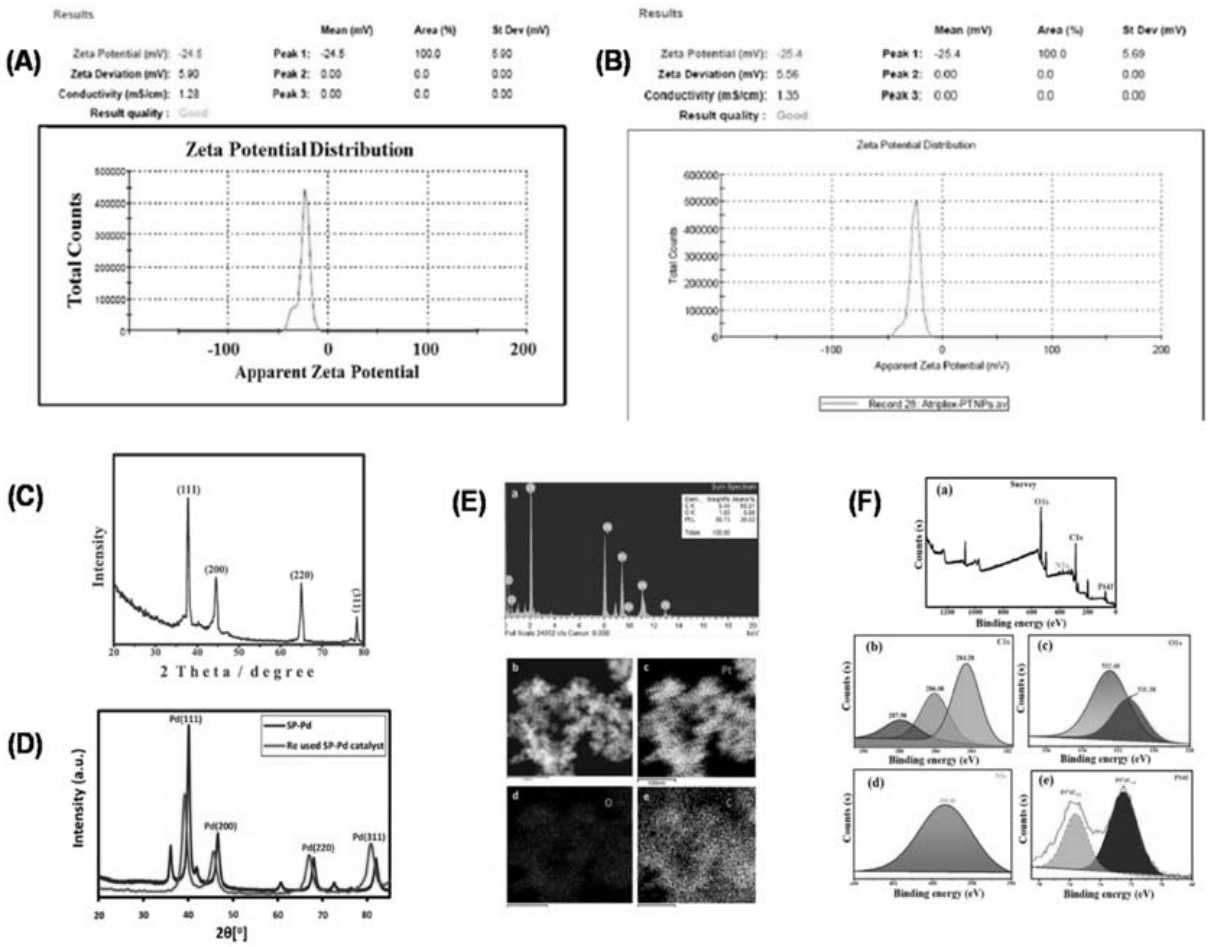

FIGURE 23.5 (A and B) Zeta potential of *Tecoma capensis* assisted synthesized AuNPs & *Atriplex halimus* leave mediated fabricated PtNPs respectively (C & D) Typical XRD diffraction pattern of *T. capensis* assisted synthesized AuNPs & *Salvadora persica* L. (sp.) mediated synthesized palladium NPs (E & F) Typical EDX of At-PtNPs (b−e) elemental mapping images and XPS spectrum of At-PtNPs (a) survey (b) C1s (c) O1s (d) N1s (e) Pt4f respectively. *Source: (A & B) Adopted from Hosny, M., Fawzy, M., El-Badry, Y.A., Hussein, E.E., Eltaweil, A.S., 2022a. Plant-assisted synthesis of gold nanoparticles for photocatalytic, anticancer, and antioxidant applications. J. Saudi Chem. Soc. 26, 101419. https://doi.org/10.1016/j.jscs.2022.101419; Hosny, M., Fawzy, M., El-Fakharany, E.M., Omer, A.M., El-Monaem, E.M.A., Khalifa, R.E., et al., 2022b. Biogenic synthesis, characterization, antimicrobial, antioxidant, antidiabetic, and catalytic applications of platinum nanoparticles synthesized from Polygonum salicifolium leaves. J. Environ. Chem. Eng. 10, 106806. https://doi.org/10.1016/j.jece.2021.106806. Eltaweil, A.S., Fawzy, M., Hosny, M., Abd El-Monaem, E.M., Tamer, T.M., Omer, A.M., 2022. Green synthesis of platinum nanoparticles using Atriplex halimus leaves for potential antimicrobial, antioxidant, and catalytic applications. Arab. J. Chem. 15, 103517. https://doi.org/10.1016/j.arabjc.2021.103517. (C & D) Adopted from Hosny, M., Fawzy, M., El-Badry, Y.A., Hussein, E.E., Eltaweil, A.S., 2022a. Plant-assisted synthesis of gold nanoparticles for photocatalytic, anticancer, and antioxidant applications. J. Saudi Chem. Soc. 26, 101419. https://doi.org/10.1016/j.jscs.2022.101419; Hosny, M., Fawzy, M., El-Fakharany, E.M., Omer, A.M., El-Monaem, E.M.A., Khalifa, R.E., et al., 2022b. Biogenic synthesis, characterization, antimicrobial, antioxidant, antidiabetic, and catalytic applications of platinum nanoparticles synthesized from Polygonum salicifolium leaves. J. Environ. Chem. Eng. 10, 106806. https://doi.org/10.1016/j.jece.2021.106806, adopted from Alahmad, A., Feldhoff, A., Bigall, N.C., Rusch, P., Scheper, T., Walter, J.-G., 2021. Hypericum perforatum L.-mediated green synthesis of silver nanoparticles exhibiting antioxidant and anticancer activities. Nanomaterials 11, 487. https://doi.org/10.3390/nano11020487. (E & F) Adopted from Eltaweil, A.S., Fawzy, M., Hosny, M., Abd El-Monaem, E.M., Tamer, T.M., Omer, A.M., 2022. Green synthesis of platinum nanoparticles using Atriplex halimus leaves for potential antimicrobial, antioxidant, and catalytic applications. Arab. J. Chem. 15, 103517. https://doi.org/10.1016/j.arabjc.2021.103517.*

size by using the Scherrer equation. Fig. 23.5(C & D) depicts a typical XRD diffraction pattern of green synthesized AuNPs and PtNPs showing major reflection at 37.81, 44.51, 64.93, and 78.29 degrees corresponding to (111), (200), (220), and (311) planes for AuNPs similarly five distinct reflections at 40.02,46.49, 68.05, 81.74 and 86.24 degrees attributes to (111), (200), (220), (311) & (222) plane of Pt NPs. Interestingly, the particle size of AuNPs was calculated by using the main peak (111) of XRD at approximately 15.42 nm and the crystalline size was close to the size range calculated by TEM analysis while for PtNPs reflection at 40.02 degrees was observed and the average particle size was calculated about 10 nm which is in agreement with the TEM results. The elemental technique of EDX & XPS analysis is used to confirm the presence of metal in a zero-valent form. As the biogenic route of synthesis has an issue of purity and oxidation state and EDX as well XPS data provides information about its composition and purity. Fig. 23.4E & F reveals a typical EDX and XPS graph of green synthesized PtNPs. The results confirmed the formation of PtNPs which are in a zero-valent oxidation state (Eltaweil et al., 2022; Hosny et al., 2022a,b; Alahmad et al., 2021).

23.7 Applications of nanoaprticles

Nanotechnology has fast become one of the most useful tools in a variety of areas like medicine, industry, electronics, agriculture, food, cosmetics, etc. The synthesized nanoparticle has shown numerous applications as presented in Fig. 23.6.

23.7.1 Applications of nanoaprticles in medicine

Nanomedicine is one of the most important areas where NPs are being used. Nanotechnology also finds applications in the diagnosis and screening of various diseases as well as in their treatment. NPs are currently under extensive research in the development of drug delivery vehicles, implants, vaccines, etc.

23.7.1.1 Anticancer activity

Cancer treatment includes chemotherapy, radiation therapy, surgery, immunotherapy, etc., all of which are associated with several side effects, as they also target healthy cells. In this context, several studies in recent years explore the role of NPs in the treatment of cancer, which would be more targeted and so, less harmful. Many NPs made from plants have demonstrated anticancer action and the most commonly used metallic NPs are gold, silver, iron and copper NPs, which have excellent optical and photothermal properties. The mechanism of the anticancer effect of NPs has mainly been found to be due to increased levels of ROS leading to oxidative stress in cancer cells which results in apoptosis, as in the case of AgNPs prepared from extracts of the cyanobacterium *Anabaena doliolum* (Singh et al., 2014). Another example is the antitumor activity of ZnONPs produced from *Cassia auriculata* leaf extract, which has no effect on healthy human breast cells but is active against MCF-7 breast cancer cells. Also, AuNPs produced from

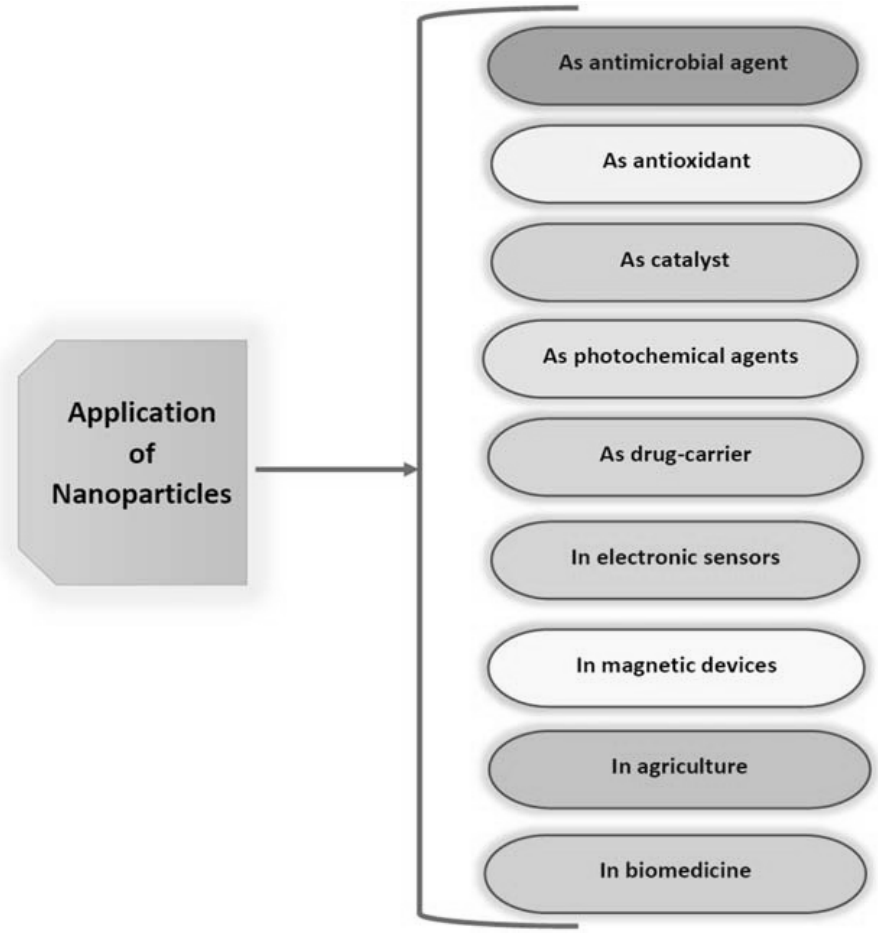

FIGURE 23.6 Application of nanoparticles in different disciplines of science and technology.

Trachyspermum ammi seed extract inhibited the growth of HepG-2 cancer cell lines, which was connected to ROS-driven cell death (Perveen et al., 2021). Another mechanism for the anticancer effect is interaction with proteins present in cancer cells. For example, longan peel powder-mediated AgNPs have been reported to exhibit in vivo and in vitro cytotoxicity in human lung cancer H1299 cells and in the mouse model, which has been attributed to the inhibition of NF-κB activity, decrease in the expression of Bcl-2/caspase-3 as well as the elevated surviving level (He et al., 2016). Several other studies on biogenic NPs advocate their potential in cancer chemotherapy. However, before an NP-based drug can be used in cancer treatment, its pharmacology and pharmacokinetics need to be thoroughly understood. Similarly, the role of NPs in cancer drug delivery systems and the fate thereafter need to be studied. *Ephedra aphylla* extract and associated SeNPs and ZnNPs were tested against six cancer celllines and a normal lung fibroblast (WI-38) cell line. The extract showed a strong cytotoxic effect against HePG-2, HCT-116 and HeLa cell lines (El-Zayat et al., 2021). The greater activity of the NPs than the plant extract may be attributed to the large surface area which enhances the efficiency of the NPs towards the inhibition of cancer cell growth.

23.7.1.2 Antileishmanial activity

Leishmaniasis, which is a protozoan-borne illness, affects millions of people worldwide. It was earlier treated with chemotherapy, which had unfavorable side effects. In recent years, a variety of nanotechnology-based techniques and products, such as liposomes, lipid nano-capsules, metal and metallic oxide NPs, polymeric NPs, nanotubes, and nanovaccines, have become antileishmanial drugs, due to their distinctive qualities, such as bioavailability, reduced toxicity, targeted drug delivery, and biodegradability. While xylan alone showed little effect, xylan-containing AgNPs (also known as nanoxylan) produced utilizing a green synthesis method using corncob xylan as a reducing and stabilizing agent effectively decreased *Leishmania amazonensis* promastigote viability (Silva Viana et al., 2020). The potential of the nanoxylan as a promising new antiparasitic drug is amply demonstrated by this investigation. In another study on ZnONPs produced from *Verbena officinalis* and *Verbena tenuisecta* plant leaf extracts, both NPs exhibited antileishmanial activity, with the *V. officinalis* ZnONPs having better activity due to the greater phenolic content and smaller size as compared to *V. tenuisecta*-mediated ZnONPs (Afridi et al., 2018).

23.7.1.3 Antimicrobial activity

Antibiotic resistance has become one of the most important challenges to the medical community in recent years. Due to various reasons, bacteria are becoming resistant to most antibiotics available, leading to issues related to the treatment and prevention of infectious diseases. Biogenic NPs may be a viable option to explore here, as they have shown promising results in treating multidrug-resistant bacteria (Nadeem et al., 2017). Nanomaterials are being used as antimicrobial agents in place of antibiotics and also to support known antibiotics by acting as carriers (Zhang et al., 2010). Due to their small size, NPs can interact more closely with bacterial cells and have a strong bactericidal effect. NPs are also able to overcome resistance mechanisms used by bacteria, such as increased efflux of drugs from the bacterial cell and biofilm formation. This is perhaps the reason why NPs are good antimicrobials and are also effective against multidrug-resistant bacteria. To boost the antibacterial response, several organic and inorganic compounds have been combined with NPs and other conjugates. Ag is well known for its antibacterial properties. Green AgNPs produced from the leaf extract of *Carissa carandas* have shown antibacterial action against a range of human pathogenic microorganisms, particularly against *Shigella flexneri* (Singh et al., 2021). Similarly, Pd-Ag NPs produced from stevia leaf extract and covered with reduced graphene oxide, have been found to limit the growth of Gram-negative bacteria like *Escherichia coli*. In another study, multidrug-resistant *Pseudomonas aeruginosa* and *Acinetobacter baumanii*, which cause ventilator-associated pneumonia, were inhibited by AgNPs derived from the Saudi Arabian desert plant *Sisymbrium irio* (Mickymaray, 2019). In a study on AgNPs derived from *Clerodendrum inerme* leaf extract, the NPs were found to show both antibacterial and antifungal activities. AuNPs made from *C. inerme* extracts also displayed similar inhibitory effects, leading to the conclusion that these NPs may have increased antibacterial activity due to the synergistic interaction of physiologically active phytochemicals present in the plant (Khan et al., 2020). AuNPs obtained from *T. amni* seed extract showed antibiofilm action against

Listeria monocytogenes and Serratia marcescens (Perveen et al., 2021). AuNPs mediated from *Galaxaura elongate* showed potential antibacterial activity against E. *coli* and *Klebsiella pneumonia* (Nadeem et al., 2017). The proteomic studies of AuNPs against *E. coli* showed a change in the expression of heat shock protein (Eom et al., 2012). CuONPs produced from *Cymbopogon citratus*, have shown considerable antibacterial action as well as antibiofilm characteristics which they believe to be attributable to changes in the cell wall compositions of the bacterial strains studied (Cherian et al., 2020). ZnONPs derived from the bark extract of *Cinnamomum verum* showed potent antimicrobialactivity against *E. coli* and *Staphylococcus aureus* (Andleeb et al., 2021). Similarly, *C. auriculata* extract was also used to derive ZnONPs which showed antibacterial activity owing to direct cell contact which disrupts the bacterial cell wall (Prasad et al., 2020). MnONPs made from the leaf extract of *Abutilon indicum* were found to be effective against both Gram-negative and Gram-positive bacteria. In addition to antibacterial activity, bio-mediated NPs have also been reported to display antifungal effects by increasing ROS. For example, FeNPs synthesized using *Acacia nilotica* seedless pods extract were found to be effective against a species of *Candida*, in addition to different bacteria (Da'na et al., 2018). Nanoxylan derived from corncob xylan has been shown to have antifungal activity against *Candida albicans, Candida parapsilosis*, and *Cryptococcus neoformans* (Silva Viana et al., 2020). Anti-viral activity of biogenic NPs has also been reported, however, it is still in the early stage of research and needs to be further studied. Plant-based NPs have indeed gained considerable importance as antimicrobial agents, however, their unique mode of action, toxicity, and potential environmental concerns associated with their use are yet to be completely understood.

23.7.1.4 Antioxidant activity

The exploration of the antioxidant potential of plant-based NPs has garnered a lot of attention, particularly in pharmaceutical science. *T. capensis* (L.) found in tropical and subtropical areas of Africa consist of several phytochemicals like flavonoids, glycosides, terpenoids and polyphenols, etc. (Kavya et al., 2015). The plant extract was used to synthesize AuNPs and its antioxidant activity was tested. The antioxidant activity was tested via DPHH (2,2-diphenyl-1-picrylhydrazyl) assay. All the samples showed inhibitory action against DPPH free radicals in a dose-dependent manner. At 100 μg/mL *T. capensis* and its AuNP extract showed 85.62% and 70.73% activity (Hosny et al., 2022). The biogenic synthesis of ZnONPs by using neem (*A. indica*) extract has been reported and the DDPH scavenging activity was investigated (Madan et al., 2016). The ZnONPs showed potent antioxidant activity with the IC_{50} value of 8355 μg/mL. The percentage of scavenging activity of the NPs was approximately 92%. The activity was attributed to the crystallite size, bullet-shaped geometry, and also due to the transfer of electron density located at oxygen to the unpaired electron located at nitrogen in DPPH which results in the decrease of intensity of $n-\pi^*$ transition (Das et al., 2013a,b). The antioxidant potential of AuNPs mediated from *Alium cepa* showed moderate antioxidant potential (Patra et al., 2016). The activity was linked to the presence of secondary metabolites in plant extract, similarly, the AuNPs obtained from avocado oil also showed an efficacy of 30.49% at 40 μL (Kumar, et al., 2018). Aqueous extract of *E. aphylla* was used to derive SeNPs and ZnNPs. The NPs were characterized by TEM and zeta potential analyses (El-Zayat et al., 2021). The plant extract and the associated NPs showed high antioxidant potential as assessed by the

DPPH assay. The tannins and flavonoids present in the extract were found to be responsible for the antioxidant activity. The presence of −OH groups in these phytoconstituents is a significant factor that makes them good reducing agents (El-Shahaby et al., 2013).

23.7.1.5 Antidiabetic activity

Antidiabetic activity of *Physalis minima*-derived AuNPs has been assessed through an alpha-amylase inhibition assay (Sekar et al., 2022). The aqueous extract of the NPs was found to suppress most alpha-amylase enzyme activity and exerted 90%−93% antidiabetic activity. Phytochemicals such as flavonoids and polyphenols were responsible for the activity and the NPs inhibited carbohydrate hydrolyzing enzyme.

23.7.1.6 Agricultural applications

Due to their small size, NPs are being used in agriculture as well, for plant nutrition, plant protection, soil remediation, processing, etc (Husen 2022). The antimicrobial action of NPs, as discussed in the preceding section, may be employed for the protection of crops against microbes and pests. ZnO and TiO_2 NPs derived from lemon fruit have demonstrated antiphytopathogenic activity against the soft rot bacteria pathogen *Dickeya dadantii* (Hossain et al., 2019). Another study on ZnONPs made using *Eucalyptus globules* extract found the fungicidal activity of the NPs against apple orchard pathogens without affecting the plants, thereby proving the advantage of biogenic NPs in agriculture (Ahmad et al., 2020a,b,c). AgNPs synthesized from wheat extract adversely affected wheat salt stress by altering abscisic acid levels, ion homeostasis, and defense mechanisms including both enzymatic and non-enzymatic antioxidants (Husen, 2022).

23.7.2 Applications of nanoparticles in bioremediation

Water pollution from sewage waste and effluents from textile, dyes, and paint industries, contains nonbiodegradable dyes and poses a serious hazard to the environment. Researchers are constantly working on developing more efficient and eco-friendly technology to counter this. NPs are proving useful in this field as well, due to their photocatalytic activity as they have a unique size, shape, and optical activity. For example, ZnONPs synthesized using leaf extract of *Plectranthus amboinicus* show better photocatalytic activity in the degradation of the dye methyl red compared to hydrothermal synthesized ZnONPs (Fu and Fu, 2015). The OH radicals formed by the photocatalytic activity of the ZnONPs react with organic and inorganic pollutants that get absorbed on the surface of ZnO and convert them to nontoxic H_2O, CO_2, and inorganic compounds (Rauf and Ashraf, 2009). Similarly, AgNPs synthesized by *Matricaria chamomilla* showed catalytic activity against the dye Rhodamine B, under UV light, and this effect may be enhanced by the phenols present in the plant extract (Alshehri and Malik, 2020). CuO NPs synthesized by *Rheum palmatum* root extract have been found to degrade the dyes rhodamine B, and methylene blue (Bordbar et al., 2017). In a study on MnONPs produced from an *A. indicum* leaf extract, in addition to their antimicrobial activity, the NPs also showed strong photocatalytic activity as well as absorption activity against the heavy metal Cr, which displays their promising potential for bioremediation of various organic and inorganic contaminants

(Khan et al., 2020). It can be concluded that biogenic NPs are an environment-friendly option for the purification of polluted water and should be further explored as a large-scale option. AuNPs have been explored as photocatalytic agents and have been found to degrade organic pollutants. The photocatalytic activity has been linked to their large surface area (Mohite et al., 2016). The catalytic effect of AuNPs derived from *M. tenuiflora* has been reported (Rodríguez-León et al., 2019). The biogenic AuNPs associated with *Trichoderma* sp. have been explored as catalytic agents in the degradation of azo dyes (Qu et al., 2017), similarly, AuNPs synthesized from *Delonix regia* leaf extract have shown potent catalytic activity (Dauthal and Mukhopadhyay, 2016). It has been found that AuNPs can induce localized surface plasmon resonance by absorbing visible light, thereby enhancing the generation and separation of electron/hole pairs in the semiconductor. In addition, AuNPs can also serve as electron sinks (Vinay et al., 2020). Fig. 23.7 summarizes the mechanistic actions of AuNPs mediated activities (Akintelu et al., 2021).

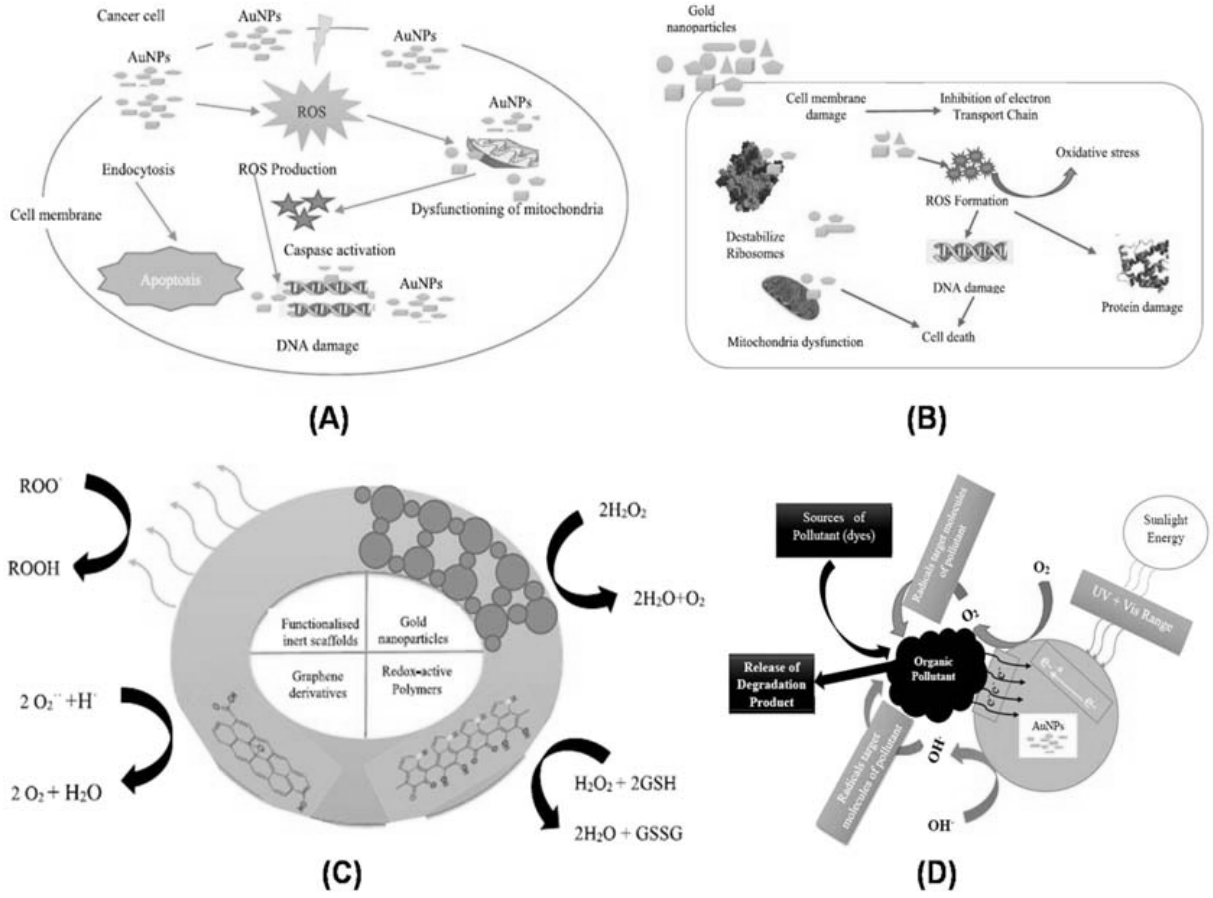

FIGURE 23.7 Diagrammatic representation of (A) anticancer activity, (B) antimicrobial activity, (C) antioxidant activity, and (D) bioremediation meditated by plant-based NPs. *Source: Adopted from Akintelu, S. A., Bo Yao, B., Folorunso, A.S., 2021. Bioremediation and pharmacological applications of gold nanoparticles synthesized from plant materials. Heliyon 7, e06591. https://doi.org/10.1016/j.heliyon.2021.e06591.*

23.8 Conclusion

The conventional synthesis to obtain NPs involves toxic chemicals which may have long-term impacts on human and environmental health. To reduce the risk, it is of utmost importance to come up with environment-friendly procedures which are also cost-effective. This approach makes the exploration of biogenic synthesis most appropriate and relevant. The present chapter has described the synthesis of different plant-based NPs having metal precursors in a comprehensive manner. Overall, this chapter summarized different metal and metal oxide-based NPs derived from different plants and their applications in different arenas. Along with the synthesis, it is also very important to characterize the synthesized NPs and the most appropriate techniques used for the purpose have been discussed in detail with suitable studies. The NPs are also associated with many applications, particularly in medicine and some of the important applications have been reviewed in the chapter. However, in the future, it is necessary to understand and disseminate the biological action of the NPs and how they impact the enzymatic reactions and biological pathways.

References

Abdelfatah, A.M., Fawzy, M., Eltaweil, A.S., El-Khouly, M.E., 2021. Green synthesis of nano-zero-valent iron using *Ricinus communis* seeds extract: characterization and application in the treatment of methylene blue-polluted water. ACS Omega 6, 25397–25411. Available from: https://doi.org/10.1021/acsomega.1c03355.

Abomuti, M.A., Danish, E.Y., Firoz, A., Hasan, N., Malik, M.A., 2021. Green synthesis of zinc oxide nanoparticles using *salvia officinalis* leaf extract and their photocatalytic and antifungal activities. Biology 10, 1075. Available from: https://doi.org/10.3390/biology10111075.

Ahmad, W., Jaiswal, Kumar, Amjad, M., K., 2020a. *Euphorbia herita* leaf extract as a reducing agent in a facile green synthesis of iron oxide nanoparticles and antimicrobial activity evaluation. Inorg. Nano-Met Chem. 1–8. Available from: https://doi.org/10.1080/24701556.2020.1815062.

Ahmad, W., Jaiswal, K.K., Soni, S., 2020b. Green synthesis of titanium dioxide (TiO_2) nanoparticles by using Mentha arvensis leaves extract and its antimicrobial properties. Inorg. Nano-Met Chem. 50, 1032–1038. Available from: https://doi:10.1080/24701556.2020.173241.

Ahmad, H., Venugopal, K., Rajagopal, K., De Britto, S., Nandini, B., Pushpalatha, H.G., et al., 2020c. Green synthesis and characterization of zinc oxide nanoparticles using eucalyptus globules and their fungicidal ability against pathogenic fungi of apple orchards. Biomolecules 10, 425. Available from: https://doi.org/10.3390/biom10030425.

Akhter, G., Khan, A., Ali, S.G., Khan, T.A., Siddiqi, K.S., Khan, H.M., 2020. Antibacterial and nematicidal properties of biosynthesized Cu nanoparticles using extract of holoparasitic plant. SN Appl. Sci. 2, 1268. Available from: https://doi.org/10.1007/s42452-020-3068-6.

Akintelu, S.A., Bo Yao, B., Folorunso, A.S., 2021. Bioremediation and pharmacological applications of gold nanoparticles synthesized from plant materials. Heliyon 7, e06591. Available from: https://doi.org/10.1016/j.heliyon.2021.e06591.

Al-Radadi, N.S., 2019. Green synthesis of platinum nanoparticles using Saudi's Dates extract and their usage on the cancer cell treatment. Arab. J. Chem. 12, 330–349. Available from: https://doi.org/10.1016/j.arabjc.2018.05.008.

Alahmad, A., Al-Zereini, W.A., Hijazin, T.J., Al-Madanat, O.Y., Alghoraibi, I., Al-Qaralleh, O., et al., 2022. Green synthesis of silver nanoparticles using *Hypericum perforatum* L. aqueous extract with the evaluation of its antibacterial activity against clinical and food pathogens. Pharmaceutics 14, 1104. Available from: https://doi.org/10.3390/pharmaceutics14051104.

Alahmad, A., Feldhoff, A., Bigall, N.C., Rusch, P., Scheper, T., Walter, J.-G., 2021. *Hypericum perforatum* L.-mediated green synthesis of silver nanoparticles exhibiting antioxidant and anticancer activities. Nanomaterials 11, 487. Available from: https://doi.org/10.3390/nano11020487.

Ali, K., Ahmed, B., Dwivedi, S., Saquib, Q., Al-Khedhairy, A.A., Musarrat, J., 2015. Microwave accelerated green synthesis of stable silver nanoparticles with eucalyptus globulus leaf extract and their antibacterial and antibiofilm activity on clinical isolates. PLOS ONE 10, e0131178. Available from: https://doi.org/10.1371/journal.pone.0131178.

Ali, S., Perveen, S., Ali, M., Jiao, T., Sharma, A.S., Hassan, H., et al., 2020. Bioinspired morphology-controlled silver nanoparticles for antimicrobial application. Mater. Sci. Eng. C 108, 110421. Available from: https://doi.org/10.1016/j.msec.2019.110421.

Alle, M., Bandi, R., Sharma, G., Dadigala R., Husen, A., Kim, J.C., 2022. Current trends in engineered gold nanoparticles for cancer therapy. In: Kim JC, Alle M, Husen A (eds) Smart Nanomaterials in Biomedical Applications. Nanotechnology in the Life Science. Springer, Cham. pp. 1–40. Available from: https://doi.org/10.1007/978-3-030-84262-8_1. ISBN: 978-3-030-84261-1.

Alshehri, A.A., Malik, M.A., 2020. Phytomediated Photo-induced green synthesis of silver nanoparticles using *Matricaria chamomilla* L. and its catalytic activity against Rhodamine B. Biomolecules 10, 1604. Available from: https://doi.org/10.3390/biom10121604.

Amina, S.J., Guo, B., 2020. A review on the synthesis and functionalization of gold nanoparticles as a drug delivery vehicle. Int. J. Nanomed. 15, 9823–9857. Available from: https://doi.org/10.2147/IJN.S279094.

Amin, M., Anwar, F., Janjua, M.R.S.A., Iqbal, M.A., Rashid, U., 2012. Green synthesis of silver nanoparticles through reduction with *Solanum xanthocarpum* L. berry extract: characterization, antimicrobial and urease inhibitory activities against Helicobacter pylori. Int. J. Mol. Sci. 13, 9923–9941.

Andleeb, Anisa, Andleeb, Aneeta, Asghar, S., Zaman, G., Tariq, M., Mehmood, A., et al., 2021. A systematic review of biosynthesized metallic nanoparticles as a promising anti-cancer-strategy. Cancers 13, 2818. Available from: https://doi.org/10.3390/cancers13112818 (Basel).

Ankamwar, B., Chaudhary, M., Sastry, M., 2005. Gold Nanotriangles biologically synthesized using tamarind leaf extract and potential application in vapor sensing. Synth. React. Inorg. Metal-Org. Nano-Metal Chem. 35, 19–26. Available from: https://doi.org/10.1081/SIM-200047527.

Ansari, A., Siddiqui, V.U., Rehman, W.U., Akram, Md.K., Siddiqi, W.A., Alosaimi, A.M., et al., 2022. Green synthesis of TiO_2 nanoparticles using acorus calamus leaf extract and evaluating its photocatalytic and in vitro antimicrobial activity. Catalysts 12, 181. Available from: https://doi.org/10.3390/catal12020181.

Armelao, L., Barreca, D., Bottaro, G., Gasparotto, A., Tondello, E., Ferroni, M., et al., 2004. Au/TiO_2 nanosystems: a combined RF-sputtering/Sol − Gel approach. Chem. Mater 16, 3331–3338. Available from: https://doi.org/10.1021/cm0353308.

Armendariz, V., Herrera, I., peralta-videa, J.R., Jose-yacaman, M., Troiani, H., Santiago, P., et al., 2004. Size controlled gold nanoparticle formation by Avena sativa biomass: use of plants in nanobiotechnology. J. Nanopart. Res. 6, 377–382. Available from: https://doi.org/10.1007/s11051-004-0741-4.

Aromal, S.A., Philip, D., 2012. *Benincasa hispida* seed mediated green synthesis of gold nanoparticles and its optical nonlinearity. Phys. E: Low-Dimens. Syst. Nanostructures 44, 1329–1334. Available from: https://doi.org/10.1016/j.physe.2012.02.013.

Aslam, M., Abdullah, A.Z., Rafatullah, M., 2021. Recent development in the green synthesis of titanium dioxide nanoparticles using plant-based biomolecules for environmental and antimicrobial applications. J. Ind. Eng. Chem. 98, 1–16. Available from: https://doi.org/10.1016/j.jiec.2021.04.010.

Aygun, A., Gülbagca, F., Ozer, L.Y., Ustaoglu, B., Altunoglu, Y.C., Baloglu, M.C., et al., 2020a. Biogenic platinum nanoparticles using black cumin seed and their potential usage as antimicrobial and anticancer agent. J. Pharm. Biomed. Anal. 179, 112961. Available from: https://doi.org/10.1016/j.jpba.2019.112961.

Aygün, A., Özdemir, S., Gülcan, M., Cellat, K., Şen, F., 2020b. Synthesis and characterization of Reishi mushroom-mediated green synthesis of silver nanoparticles for the biochemical applications. J. Pharm. Biomed. Anal. 178, 112970. Available from: https://doi.org/10.1016/j.jpba.2019.112970.

Bachheti, R.K., Gupta, V., Husen, A., Joshi, A., Konwarh, R., 2019a. Green synthesis of iron oxide nanoparticles: cutting edge technology and multifaceted applications. In: Husen, A., Iqbal, M. (Eds.), Nanomaterials and Plant Potential. Springer International Publishing AG, Cham, pp. 239–259. Available from: https://doi.org/10.1007/978-3-030-05569-1_9.

Bachheti, A., Sharma, A., Bachheti, R.K., Husen, A., Pandey, D.P., 2019b. Plant allelochemicals and their various applications. In: Merillon, J.-M., Ramawat, K.G. (Eds.), Co-Evolution of Secondary Metabolites, Reference Series in Phytochemistry. Springer International Publishing, Cham, pp. 1–25. Available from: https://doi.org/10.1007/978-3-319-76887-8_14-1.

Banerjee, J., Narendhirakannan, R.T., 2011. Biosynthesis of silver nanoparticles from *Syzygium cumini* (L.) seed extract and evaluation of their in vitro antioxidant activities. Dig. J. Nanomater Biostructur. 6, 961–968.

Bar, H., Bhui, D.Kr, Sahoo, G.P., Sarkar, P., De, S.P., Misra, A., 2009. Green synthesis of silver nanoparticles using latex of Jatropha curcas. Colloids Surf. A: Physicochem. Eng. Asp. 339, 134–139. Available from: https://doi.org/10.1016/j.colsurfa.2009.02.008.

Bayrami, A., Haghgooie, S., Rahim Pouran, S., Mohammadi Arvanag, F., Habibi-Yangjeh, A., 2020. Synergistic antidiabetic activity of ZnO nanoparticles encompassed by *Urtica dioica* extract. Adv. Powder Technol. 31, 2110–2118. Available from: https://doi.org/10.1016/j.apt.2020.03.004.

Bekele, E.T., Gonfa, B.A., Zelekew, O.A., Belay, H.H., Sabir, F.K., 2020. Synthesis of titanium oxide nanoparticles using root extract of *Kniphofia foliosa* as a template, characterization, and its application on drug resistance bacteria. J. Nanomater. 2020, 1–10. Available from: https://doi.org/10.1155/2020/2817037.

Benassai, E., Del Bubba, M., Ancillotti, C., Colzi, I., Gonnelli, C., Calisi, N., et al., 2021. Green and cost-effective synthesis of copper nanoparticles by extracts of nonedible and waste plant materials from Vaccinium species: characterization and antimicrobial activity. Mater. Sci. Eng. C. 119, 111453. Available from: https://doi.org/10.1016/j.msec.2020.111453.

Boomi, P., Poorani, G.P., Selvam, S., Palanisamy, S., Jegatheeswaran, S., Anand, K., et al., 2020. Green biosynthesis of gold nanoparticles using *Croton sparsiflorus leaves* extract and evaluation of UV protection, antibacterial and anticancer applications. Appl. Organomet. Chem. 34. Available from: https://doi.org/10.1002/aoc.5574.

Bordbar, M., Sharifi-Zarchi, Z., Khodadadi, B., 2017. Green synthesis of copper oxide nanoparticles/clinoptilolite using *Rheum palmatum* L. root extract: high catalytic activity for reduction of 4-nitro phenol, rhodamine B, and methylene blue. J. Sol-Gel Sci. Technol. 81, 724–733. Available from: https://doi.org/10.1007/s10971-016-4239-1.

Botteon, C.E.A., Silva, L.B., Ccana-Ccapatinta, G.V., Silva, T.S., Ambrosio, S.R., Veneziani, R.C.S., et al., 2021. Biosynthesis and characterization of gold nanoparticles using Brazilian red propolis and evaluation of its antimicrobial and anticancer activities. Sci. Rep. 11, 1974. Available from: https://doi.org/10.1038/s41598-021-81281-w.

Brumbaugh, A.D., Cohen St., K.A., Angelo, S.K., 2014. Ultrasmall copper nanoparticles synthesized with a plant tea reducing agent. ACS Sustain. Chem. Eng. 2, 1933–1939. Available from: https://doi.org/10.1021/sc500393t.

Buarki, F., AbuHassan, H., Al Hannan, F., Henari, F.Z., 2022. Green synthesis of iron oxide nanoparticles using *Hibiscus rosa sinensis* flowers and their antibacterial activity. J. Nanotechnol. 2022, 1–6. Available from: https://doi.org/10.1155/2022/5474645.

Buniyamin, I., Akhir, R.M., Asli, N.A., Khusaimi, Z., Rusop, M., 2022. Green synthesis of tin oxide nanoparticles by using leaves extract of *Chromolaena Odorata*: the effect of different thermal calcination temperature to the energy band gap. Mater. Today: Proc. 48, 1805–1809. Available from: https://doi.org/10.1016/j.matpr.2021.09.117.

Chandra, C., Khan, F., 2020. Nano-scale zerovalent copper: green synthesis, characterization and efficient removal of uranium. J. Radioanal. Nucl. Chem. 324, 589–597. Available from: https://doi.org/10.1007/s10967-020-07080-1.

Cherian, T., Ali, K., Saquib, Q., Faisal, M., Wahab, R., Musarrat, J., 2020. *Cymbopogon citratus* functionalized green synthesis of CuO-nanoparticles: novel prospects as antibacterial and antibiofilm agents. Biomolecules 10, E169. Available from: https://doi.org/10.3390/biom10020169.

Chouhan, D., Mandal, P., 2021. Applications of chitosan and chitosan based metallic nanoparticles in agrosciences-a review. Int. J. Biol. Macromol. 166, 1554–1569. Available from: https://doi.org/10.1016/j.ijbiomac.2020.11.035.

Costa-Coquelard, C., Schaming, D., Lampre, I., Ruhlmann, L., 2008. Photocatalytic reduction of Ag_2SO_4 by the Dawson anion α-[P2W18O62]6 − and tetracobalt sandwich complexes. Appl. Catal. B: Environ. 84, 835–842. Available from: https://doi.org/10.1016/j.apcatb.2008.06.018.

Das, R.K., Gogoi, N., Bora, U., 2011. Green synthesis of gold nanoparticles using Nyctanthes arbortristis flower extract. Bioprocess. Biosyst. Eng. 34, 615–619. Available from: https://doi.org/10.1007/s00449-010-0510-y.

Das, D., Nath, B.C., Phukon, P., Dolui, S.K., 2013a. Synthesis and evaluation of antioxidant and antibacterial behavior of CuO nanoparticles. Colloids Surf. B Biointerfaces 101, 430–433. Available from: https://doi.org/10.1016/j.colsurfb.2012.07.002.

Das, D., Nath, B.C., Phukon, P., kalita, A., Dolui, S.K., 2013b. Synthesis of ZnO nanoparticles and evaluation of antioxidant and cytotoxic activity. Colloids Surf. B: Biointerfaces 111, 556–560. Available from: https://doi.org/10.1016/j.colsurfb.2013.06.041.

Dauthal, P., Mukhopadhyay, M., 2016. Phyto-synthesis and structural characterization of catalytically active gold nanoparticles biosynthesized using Delonix regia leaf extract. 3 Biotech. 6, 118. Available from: https://doi.org/10.1007/s13205-016-0432-8.

Davids, J.S., Ackah, M., Okoampah, E., Fometu, S.S., Guohua, W., Jianping, Z., 2021. Biocontrol of bacteria associated with pinewiltnematode, bursaphelenchus xylophilus by using plant mediated gold nanoparticles. Int. J. Agric. Biol. 26, 517–526. Available from: https://doi.org/10.17957/IJAB/15.1863.

Da'na, E., Taha, A., Afkar, E., 2018. Green synthesis of iron nanoparticles by acacia nilotica pods extract and its catalytic, adsorption, and antibacterial activities. Appl. Sci. 8, 1922. Available from: https://doi.org/10.3390/app8101922.

Dhamecha, D., Jalalpure, S., Jadhav, K., 2016. Nepenthes khasiana mediated synthesis of stabilized gold nanoparticles: characterization and biocompatibility studies. J. Photochem. Photobiol. B: Biol. 154, 108–117. Available from: https://doi.org/10.1016/j.jphotobiol.2015.12.002.

Din, M.I., Arshad, F., Hussain, Z., Mukhtar, M., 2017. Green adeptness in the synthesis and stabilization of copper nanoparticles: catalytic, antibacterial, cytotoxicity, and antioxidant activities. Nanoscale Res. Lett. 12, 638. Available from: https://doi.org/10.1186/s11671-017-2399-8.

Doan, V.-D., Thieu, A.T., Nguyen, T.-D., Nguyen, V.-C., Cao, X.-T., Nguyen, T.L.-H., et al., 2020. Biosynthesis of gold nanoparticles using *Litsea cubeba* fruit extract for catalytic reduction of 4-nitrophenol. J. Nanomater. 2020, 1–10. Available from: https://doi.org/10.1155/2020/4548790.

Dobrucka, R., 2017. Synthesis of titanium dioxide nanoparticles using *Echinacea purpurea* herba. Iran. J. Pharm. Res. IJPR 16, 756–762.

Dong, L., Li, R., Wang, Liqiu, Lan, X., Sun, H., Zhao, Y., et al., 2021. Green synthesis of platinum nanoclusters using lentinan for sensitively colorimetric detection of glucose. Int. J. Biol. Macromol. 172, 289–298. Available from: https://doi.org/10.1016/j.ijbiomac.2021.01.049.

Dubey, S.P., Lahtinen, M., Sillanpaa, M., 2010. Tansy fruit mediated greener synthesis of silver and gold nanoparticles. Process. Biochem. 45, 1065–1071.

Dwivedi, A.D., Gopal, K., 2010. Biosynthesis of silver and gold nanoparticles using *Chenopodium album* leaf extract. Colloids Surf A Physicochem. Eng. Asp. 369, 27–33.

El-Borady, O.M., Fawzy, M., Hosny, M., 2021. Antioxidant, anticancer and enhanced photocatalytic potentials of gold nanoparticles biosynthesized by common reed leaf extract. Appl. Nanosci. Available from: https://doi.org/10.1007/s13204-021-01776-w.

El-Zayat, M.M., Eraqi, M.M., Alrefai, H., El-Khateeb, A.Y., Ibrahim, M.A., Aljohani, H.M., et al., 2021. The antimicrobial, antioxidant, and anticancer activity of greenly synthesized selenium and zinc composite nanoparticles using *Ephedra aphylla* extract. Biomolecules 11, 470. Available from: https://doi.org/10.3390/biom11030470.

Eltaweil, A.S., Fawzy, M., Hosny, M., Abd El-Monaem, E.M., Tamer, T.M., Omer, A.M., 2022. Green synthesis of platinum nanoparticles using *Atriplex halimus* leaves for potential antimicrobial, antioxidant, and catalytic applications. Arab. J. Chem. 15, 103517. Available from: https://doi.org/10.1016/j.arabjc.2021.103517.

Eom, S.-H., Kim, Y.-M., Kim, S.-K., 2012. Antimicrobial effect of phlorotannins from marine brown algae. Food Chem. Toxicol. 50, 3251–3255. Available from: https://doi.org/10.1016/j.fct.2012.06.028.

Fadeel, B., Garcia-Bennett, A.E., 2010. Better safe than sorry: understanding the toxicological properties of inorganic nanoparticles manufactured for biomedical applications. Adv. Drug. Deliv. Rev. 62, 362–374. Available from: https://doi.org/10.1016/j.addr.2009.11.008.

Fan, L., Ji, X., Lin, G., Liu, K., Chen, S., Ma, G., et al., 2021. Green synthesis of stable platinum nanoclusters with enhanced peroxidase-like activity for sensitive detection of glucose and glutathione. Microchem. J. 166, 106202. Available from: https://doi.org/10.1016/j.microc.2021.106202.

Fu, L., Fu, Z., 2015. Plectranthus amboinicus leaf extract–assisted biosynthesis of ZnO nanoparticles and their photocatalytic activity. Ceram. Int. 41, 2492–2496. Available from: https://doi.org/10.1016/j.ceramint.2014.10.069.

Gardea-Torresdey, J.L., Gomez, E., Peralta-Videa, J.R., Parsons, J.G., Troiani, H., Jose-Yacaman, M., 2003. Alfalfa sprouts: a natural source for the synthesis of silver nanoparticles. Langmuir 19, 1357–1361. Available from: https://doi.org/10.1021/la020835i.

Gardea-Torresdey, J.L., Parsons, J.G., Gomez, E., Peralta-Videa, J., Troiani, H.E., Santiago, P., et al., 2002. Formation and growth of Au nanoparticles inside live alfalfa plants. Nano Lett. 2, 397–401. Available from: https://doi.org/10.1021/nl015673.

Ghodake, G.S., Deshpande, N.G., Lee, Y.P., Jin, E.S., 2010. Pear fruit extract-assisted room-temperature biosynthesis of gold nanoplates. Colloids Surf. B 75, 584–589.

Ghoreishi, S.M., Behpour, M., Khayatkashani, M., 2011. Green synthesis of silver and gold nanoparticles using *Rosa damascena* and its primary application in electrochemistry. Phys. E: Low-Dimens. Syst. Nanostruct. 44, 97–104. Available from: https://doi.org/10.1016/j.physe.2011.07.008.

Ghosh, N.S., Pandey, E., Giilhotra, R.M., Singh, R., 2020. Biosynthesis of gold nanoparticles using leaf extract of *Desmodium gangeticum* and their antioxidant activity. Res. J. Pharm. Technol. 13, 2685. Available from: https://doi.org/10.5958/0974-360X.2020.00477.1.

Ghosh, S., Patil, S., Ahire, M., Kitture, R., Kale, S., Pardesi, K., et al., 2012. Synthesis of silver nanoparticles using *Dioscorea bulbifera* tuber extract and evaluation of its synergistic potential in combination with antimicrobial agents. Int. J. Nanomed. 7, 483.

Gul, R., Jan, H., Lalay, G., Andleeb, A., Usman, H., Zainab, R., et al., 2021. Medicinal plants and biogenic metal oxide nanoparticles: a paradigm shift to treat alzheimer's disease. Coatings 11, 717. Available from: https://doi.org/10.3390/coatings11060717.

Gur, T., Meydan, I., Seckin, H., Bekmezci, M., Sen, F., 2022. Green synthesis, characterization and bioactivity of biogenic zinc oxide nanoparticles. Environ. Res. 204, 111897. Available from: https://doi.org/10.1016/j.envres.2021.111897.

Hano, C., Abbasi, B.H., 2021. Plant-based green synthesis of nanoparticles: production, characterization and applications. Biomolecules 12, 31. Available from: https://doi.org/10.3390/biom12010031.

Haseena, S., Shanavas, S., Ahamad, T., Alshehri, S.M., Baskaran, P., Duraimurugan, J., et al., 2021. Investigation on photocatalytic activity of bio-treated α-Fe2O3 nanoparticles using *Phyllanthus niruri* and Moringa stenopetala leaf extract against methylene blue and phenol molecules: kinetics, mechanism and stability. J. Environ. Chem. Eng. 9, 104996. Available from: https://doi.org/10.1016/j.jece.2020.104996.

Haverkamp, R.G., Marshall, A.T., 2009. The mechanism of metal nanoparticle formation in plants: limits on accumulation. J. Nanopart. Res. 11, 1453–1463. Available from: https://doi.org/10.1007/s11051-008-9533-6.

He, Y., Du, Z., Ma, S., Liu, Y., Li, D., Huang, H., et al., 2016. Effects of green-synthesized silver nanoparticles on lung cancer cells in vitro and grown as xenograft tumors in vivo. IJN 1879. Available from: https://doi.org/10.2147/IJN.S10369.

Hong, F., Zhou, J., Liu, C., Yang, F., Wu, C., Zheng, L., et al., 2005. Effect of nano-TiO_2 on photochemical reaction of chloroplasts of Spinach. BTER 105, 269–280. Available from: https://doi.org/10.1385/BTER:105:1-3:269.

Hosny, M., Fawzy, M., 2021. Instantaneous phytosynthesis of gold nanoparticles via *Persicaria salicifolia* leaf extract, and their medical applications. Adv. Powder Technol. 32, 2891–2904. Available from: https://doi.org/10.1016/j.apt.2021.06.004.

Hosny, M., Fawzy, M., El-Badry, Y.A., Hussein, E.E., Eltaweil, A.S., 2022a. Plant-assisted synthesis of gold nanoparticles for photocatalytic, anticancer, and antioxidant applications. J. Saudi Chem. Soc. 26, 101419. Available from: https://doi.org/10.1016/j.jscs.2022.101419.

Hosny, M., Fawzy, M., El-Fakharany, E.M., Omer, A.M., El-Monaem, E.M.A., Khalifa, R.E., et al., 2022b. Biogenic synthesis, characterization, antimicrobial, antioxidant, antidiabetic, and catalytic applications of platinum nanoparticles synthesized from Polygonum salicifolium leaves. J. Environ. Chem. Eng. 10, 106806. Available from: https://doi.org/10.1016/j.jece.2021.106806.

Hossain, A., Abdallah, Y., Ali, M.A., Masum, M.M.I., Li, B., Sun, G., et al., 2019. Lemon-fruit-based green synthesis of zinc oxide nanoparticles and titanium dioxide nanoparticles against soft rot bacterial pathogen Dickeya dadantii. Biomolecules 9, E863. Available from: https://doi.org/10.3390/biom9120863.

Husen, A., 2019. Natural product-based fabrication of zinc oxide nanoparticles and their application. In: Husen, A., Iqbal, M. (Eds.), Nanomaterials and Plant Potential. Springer International Publishing AG, Cham, pp. 193–291. Available from: https://doi.org/10.1007/978-3-030-05569-1_7.

Husen, A., 2020. Introduction and techniques in nanomaterials formulation. In: Husen, A., Jawaid, M. (Eds.), Nanomaterials for Agriculture and Forestry Applications. Elsevier Inc, Cambridge, MA, pp. 1–14. Available from: https://doi.org/10.1016/B978-0-12-817852-2.00001-9.

Husen, A., Jawaid, M., 2020. Nanomaterials for Agriculture and Forestry Applications. Elsevier Inc, Cambridge, MA. Available from: https://doi.org/10.1016/C2018-0-02349-X.

Husen, A., 2022. Engineered Nanomaterials for Sustainable Agricultural Production, Soil Improvement and Stress Management. Elsevier Inc, Cambridge, MA.

Husen, A., Rahman, Q.I., Iqbal, M., Yassin, M.O., Bachheti, R.K., 2019. Plant-mediated fabrication of gold nanoparticles and their applications. In: Husen, A., Iqbal, M. (Eds.), Nanomaterials and Plant Potential. Springer International Publishing, Cham, pp. 71–110. Available from: https://doi.org/10.1007/978-3-030-05569-1_3.

Husen, A., Siddiqi, K.S., 2014. Phytosynthesis of nanoparticles: concept, controversy and application. Nanoscale Res. Lett. 9 (229), 1–24. Available from: https://doi.org/10.1186/1556-276X-9-229.

Ismail, E., Diallo, A., Khenfouch, M., Dhlamini, S.M., Maaza, M., 2016. RuO_2 nanoparticles by a novel green process via *Aspalathus linearis* natural extract & their water splitting response. J. Alloy Compd. 662, 283–289. Available from: https://doi.org/10.1016/j.jallcom.2015.11.234.

Jalill, R.D.H.A., Nuaman, R.S., Abd, A.N., 2016. Biological synthesis of Titanium Dioxide nanoparticles by *Curcuma longa* plant extract and study its biological properties. World Sci. N. 49, 204–222.

Jameel, M.S., Aziz, A.A., Dheyab, M.A., 2020. Comparative analysis of platinum nanoparticles synthesized using sonochemical-assisted and conventional green methods. Nano-Struct. Nano-Objects 23, 100484. Available from: https://doi.org/10.1016/j.nanoso.2020.100484.

Jayachandran, A., Aswathy, T.R., Nair, A.S., 2021. Green synthesis and characterization of zinc oxide nanoparticles using Cayratia pedata leaf extract. Biochem. Biophys. Rep. 26, 100995. Available from: https://doi.org/10.1016/j.bbrep.2021.100995.

Jeevanandam, J., Chan, Y.S., Danquah, M.K., 2016. Biosynthesis of metal and metal oxide nanoparticles. ChemBioEng Rev. 3, 55–67. Available from: https://doi.org/10.1002/cben.201500018.

Jeyarani, S., Vinita, N.M., Puja, P., Senthamilselvi, S., Devan, U., Velangani, A.J., et al., 2020. Biomimetic gold nanoparticles for its cytotoxicity and biocompatibility evidenced by fluorescence-based assays in cancer (MDA-MB-231) and noncancerous (HEK-293) cells. J. Photochem. Photobiol. B 202, 111715. Available from: https://doi.org/10.1016/j.jphotobiol.2019.111715.

Jha, A.K., Prasad, K., 2011. Biosynthesis of gold nanoparticles using bael (*Aegle marmelos*) leaf: mythology meets technology. Int. J. Green. Nanotechnol. 3, 92–97. Available from: https://doi.org/10.1080/19430892.2011.574560.

Jiang, H., Manolache, S., Wong, A.C.L., Denes, F.S., 2004. Plasma-enhanced deposition of silver nanoparticles onto polymer and metal surfaces for the generation of antimicrobial characteristics. J. Appl. Polym. Sci. 93, 1411–1422. Available from: https://doi.org/10.1002/app.20561.

Jin-Chul, K., Madhusudhan, A., Husen, A., 2021. Smart Nanomaterials in Biomedical Applications. Springer Nature Switzerland AG, Cham, Switzerland. Available from: https://doi.org/10.1007/978-3-030-84262-8.

Joshi, A., Sharma, A., Bachheti, R.K., Husen, A., Mishra, V.K., 2019. Plant-mediated synthesis of copper oxide nanoparticles and their biological applications. In: Husen, A., Iqbal, M. (Eds.), Nanomaterials and Plant Potential. Springer International Publishing AG, Cham, pp. 221–237. Available from: https://doi.org/10.1007/978-3-030-05569-1_8.

Kasthuri, J., Kathiravan, K., Rajendiran, N., 2009. Phyllanthin-assisted biosynthesis of silver and gold nanoparticles: a novel biological approach. J. Nanopart. Res. 11, 1075–1085. Available from: https://doi.org/10.1007/s11051-008-9494-9.

Kavya, I., Kumar, S.K., Sandhya, D., Janaki, P., Kumar, A.R., Eswaraiah, M.C., 2015. Phytochemical evaluation of Cassia tora, Caeselpinia bonducela, *Tecoma capensis*. Indian J. Res. Pharm. Biotechnol. 3, 410–412.

Kazlagić, A., Abud, O.A., Ćibo, M., Hamidović, S., Borovac, B., Omanović-Mikličanin, E., 2020. Green synthesis of silver nanoparticles using apple extract and its antimicrobial properties. Health Technol. 10, 147–150. Available from: https://doi.org/10.1007/s12553-019-00378-5.

Keshari, A.K., Srivastava, R., Singh, P., Yadav, V.B., Nath, G., 2020. Antioxidant and antibacterial activity of silver nanoparticles synthesized by *Cestrum nocturnum*. J. Ayurveda Integr. Med. 11, 37–44. Available from: https://doi.org/10.1016/j.jaim.2017.11.003.

Khalil, M.M.H., Ismail, E.H., El-Baghdady, K.Z., Mohamed, D., 2014. Green synthesis of silver nanoparticles using olive leaf extract and its antibacterial activity. Arab. J. Chem. 7, 1131–1139. Available from: https://doi.org/10.1016/j.arabjc.2013.04.007.

Khan, Mujeeb, Albalawi, G.H., Shaik, M.R., Khan, Merajuddin, Adil, S.F., Kuniyil, M., et al., 2017. Miswak mediated green synthesized palladium nanoparticles as effective catalysts for the Suzuki coupling reactions in aqueous media. J. Saudi Chem. Soc. 21, 450–457. Available from: https://doi.org/10.1016/j.jscs.2016.03.008.

Khan, M., Khan, M., Adil, S.F., Tahir, M.N., Tremel, W., Alkhathlan, H.Z., et al., 2013. Green synthesis of silver nanoparticles mediated by *Pulicaria glutinosa* extract. Int. J. Nanomed. 8, 1507–1516.

Khan, S.A., Shahid, S., Shahid, B., Fatima, U., Abbasi, S.A., 2020. Green synthesis of MnO nanoparticles using *abutilon indicum* leaf extract for biological, photocatalytic, and adsorption activities. Biomolecules 10, 785. Available from: https://doi.org/10.3390/biom10050785.

Kharey, P., Dutta, S.B., Gorey, A., Manikandan, M., Kumari, A., Vasudevan, S., et al., 2020. *Pimenta dioica* mediated biosynthesis of gold nanoparticles and evaluation of its potential for theranostic applications. ChemistrySelect 5, 7901–7908. Available from: https://doi.org/10.1002/slct.202001230.

Kuang, Y., Wang, Q., Chen, Z., Megharaj, M., Naidu, R., 2013. Heterogeneous Fenton-like oxidation of monochlorobenzene using green synthesis of iron nanoparticles. J. Colloid Interface Sci. 410, 67–73. Available from: https://doi.org/10.1016/j.jcis.2013.08.020.

Kulkarni, V., Suryawanshi, S., Kulkarni, P., 2015. Biosynthesis of copper nanoparticles using aqueous extract of Eucalyptus sp. plant leaves. Curr. Sci. 109, 255–257.

Kumari, M.M., Philip, D., 2015. Synthesis of biogenic SnO_2 nanoparticles and evaluation of thermal, rheological, antibacterial and antioxidant activities. Powder Technol. 270, 312–319.

Kumar, C.R.R., Betageri, V.S., Nagaraju, G., Suma, B.P., Kiran, M.S., Pujar, G.H., et al., 2020. One-pot synthesis of ZnO nanoparticles for nitrite sensing, photocatalytic and antibacterial studies. J. Inorg. Organomet. Polym. Mater. 30, 3476–3486. Available from: https://doi.org/10.1007/s10904-020-01544-3.

Kumar, A., Choudhary, A., Kaur, H., Guha, S., Mehta, S., Husen, A., 2022. Potential applications of engineered nanoparticles in plant disease management: a critical update. Chemosphere 295, 133798. Available from: https://doi.org/10.1016/j.chemosphere.2022.133798.

Kumar, A., Choudhary, A., Kaur, H., Mehta, S., Husen, A., 2021a. Metal-based nanoparticles, sensors and their multifaceted application in food packaging. J. Nanobiotechnol. 19, 256. Available from: https://doi.org/10.1186/s12951-021-00996-0.

Kumar, A., Choudhary, A., Kaur, H., Mehta, S., Husen, A., 2021b. Smart nanomaterial and nanocomposite with advanced agrochemical activities. Nano Res. Lett. 16, 156. Available from: https://doi.org/10.1186/s11671-021-03612-0.

Kumar, K.M., Mandal, B.K., Sinha, M., Krishnakumar, V., 2012. *Terminalia chebula* mediated green and rapid synthesis of gold nanoparticles. Spectrochim. Acta A Mol. Biomol. Spectrosc. 86, 490–494.

Kumar, P.P.N.V., Shameem, U., Kollu, P., Kalyani, R.L., Pammi, S.V.N., 2015. Green synthesis of copper oxide nanoparticles using aloe vera leaf extract and its antibacterial activity against fish bacterial pathogens. BioNanoScience 5, 135–139. Available from: https://doi.org/10.1007/s12668-015-0171-z.

Kumar, B., Smita, K., Cumbal, L., Debut, A., Galeas, S., Guerrero, V.H., 2016. Phytosynthesis and photocatalytic activity of magnetite (Fe3O4) nanoparticles using the Andean blackberry leaf. Mater. Chem. Phys. 179, 310–315. Available from: https://doi.org/10.1016/j.matchemphys.2016.05.045.

Kumar, B., Smita, K., Debut, A., Cumbal, L., 2018. Utilization of Persea americana (Avocado) oil for the synthesis of gold nanoparticles in sunlight and evaluation of antioxidant and photocatalytic activities. Environ. Nanotechnol. Monit. Manag. 10, 231–237. Available from: https://doi.org/10.1016/j.enmm.2018.07.009.

Kumar, S.S., Venkateswarlu, P., Rao, V.R., Rao, G.N., 2013. Synthesis, characterization and optical properties of zinc oxide nanoparticles. Int. Nano Lett. 3, 30. Available from: https://doi.org/10.1186/2228-5326-3-30.

Kumar, V., Yadav, S.K., 2011. Synthesis of stable, polyshaped silver, and gold nanoparticles using leaf extract of *Lonicera japonica* L. Int. J. Green. Nanotechnol. 3, 281–291. Available from: https://doi.org/10.1080/19430892.2011.633474.

Lee, Y.W., Kim, M., Kim, Z.H., Han, S.W., 2009. One-step synthesis of Au@Pd core-shell nanooctahedron. J. Am. Chem. Soc. 131, 17036–17037. Available from: https://doi.org/10.1021/ja905603p.

Lee, K.X., Shameli, K., Mohamad, S.E., Yew, Y.P., Mohamed Isa, E.D., Yap, H.-Y., et al., 2019. Bio-mediated synthesis and characterisation of silver nanocarrier, and its potent anticancer action. Nanomaterials 9, E1423. Available from: https://doi.org/10.3390/nano9101423 (Basel).

Lee, H.-J., Song, J.Y., Kim, B.S., 2013. Biological synthesis of copper nanoparticles using*Magnolia kobus* leaf extract and their antibacterial activity: biological synthesis of copper nanoparticles using *Magnoliakobus* leaf extract. J. Chem. Technol. Biotechnol. n/a-n/a. Available from: https://doi.org/10.1002/jctb.4052.

Liu, L., Jing, Y., Guo, A., Li, X., Li, Q., Liu, W., et al., 2022. Biosynthesis of platinum nanoparticles with cordyceps flower extract: characterization, antioxidant activity and antibacterial activity. Nanomaterials 12, 1904. Available from: https://doi.org/10.3390/nano12111904.

Lopez, M.L., Gardea-Torresdey, J.L., Peralta-Videa, J.R., de la Rosa, G., Armendariz, V., Herrera, I., et al., 2005. Gold binding by native and chemically modified hopbiomasses. Bioinorg. Chem. Appl. 3, 29–41.

Madan, H.R., Sharma, S.C., Udayabhanu, null, Suresh, D., Vidya, Y.S., Nagabhushana, H., et al., 2016. Facile green fabrication of nanostructure ZnO plates, bullets, flower, prismatic tip, closed pine cone: their antibacterial, antioxidant, photoluminescent and photocatalytic properties. Spectrochim. Acta A Mol. Biomol. Spectrosc. 152, 404–416. Available from: https://doi.org/10.1016/j.saa.2015.07.067.

Majeed, A., Ullah, W., Anwar, A.W., Shuaib, A., Ilyas, U., Khalid, P., et al., 2018. Cost-effective biosynthesis of silver nanoparticles using different organs of plants and their antimicrobial applications: a review. Mater. Technol. 33, 313–320. Available from: https://doi.org/10.1080/10667857.2015.1108065.

Manjare, S.B., Chaudhari, R.A., 2020. Palladium nanoparticle-bentonite hybrid using leaves of *Syzygium aqueum* plant from india: design and assessment in the catalysis of −C−C− Coupling Reaction. Chem. Afr. 3, 329–341. Available from: https://doi.org/10.1007/s42250-020-00139-2.

Maria, B.S., Devadiga, A., Kodialbail, V.S., Saidutta, M.B., 2015. Synthesis of silver nanoparticles using medicinal *Zizyphus xylopyrus* bark extract. Appl. Nanosci. 5, 755–762.

Matinise, N., Fuku, X.G., Kaviyarasu, K., Mayedwa, N., Maaza, M., 2017. ZnO nanoparticles via Moringa oleifera green synthesis: physical properties & mechanism of formation. Appl. Surf. Sci. 406, 339–347. Available from: https://doi.org/10.1016/j.apsusc.2017.01.219.

Md Ishak, N.A.I., Kamarudin, S.K., Timmiati, S.N., 2019. Green synthesis of metal and metal oxide nanoparticles via plant extracts: an overview. Mater. Res. Express 6, 112004. Available from: https://doi.org/10.1088/2053-1591/ab4458.

Mehdizadeh, T., Zamani, A., Abtahi Froushani, S.M., 2020. Preparation of Cu nanoparticles fixed on cellulosic walnut shell material and investigation of its antibacterial, antioxidant and anticancer effects. Heliyon 6, e03528. Available from: https://doi.org/10.1016/j.heliyon.2020.e03528.

Mickymaray, 2019. One-step synthesis of silver nanoparticles using Saudi Arabian desert seasonal plant *Sisymbrium irio* and antibacterial activity against multidrug-resistant bacterial strains. Biomolecules 9, 662. Available from: https://doi.org/10.3390/biom9110662.

Mishra, V.K., Husen, A., Rahman, Q.I., Iqbal, M., Sohrab, S.S., Yassin, M.O., et al., 2019. Plant-based fabrication of silver nanoparticles and their application. In: Husen, A., Iqbal, M. (Eds.), Nanomaterials and Plant Potential. Springer International Publishing AG, Cham, pp. 135–175. Available from: https://doi.org/10.1007/978-3-030-05569-1_5.

Modena, M.M., Rühle, B., Burg, T.P., Wuttke, S., 2019. Nanoparticle characterization: what to measure? Adv. Mater. 1901556. Available from: https://doi.org/10.1002/adma.201901556.

Mohan Bhagyaraj, S., Oluwafemi, O.S., 2018. Nanotechnology: the science of the invisible. Synthesis of Inorganic Nanomaterials 1–18. Available from: https://doi.org/10.1016/B978-0-08-101975-7.00001-4. Elsevier.

Mohite, P., Apte, M., Kumar, A.R., Zinjarde, S., 2016. Biogenic nanoparticles from schwanniomyces occidentalis NCIM 3459: mechanistic aspects and catalytic applications. Appl. Biochem. Biotechnol. 179, 583–596. Available from: https://doi.org/10.1007/s12010-016-2015-x.

Mukherjee, P., Senapati, S., Mandal, D., Ahmad, A., Khan, M.I., Kumar, R., et al., 2002. Extracellular synthesis of gold nanoparticles by the fungus *Fusarium oxysporum*. Chembiochem 3, 461–463.

Murthy, H.C.A., Desalegn, T., Kassa, M., Abebe, B., Assefa, T., 2020. Synthesis of green copper nanoparticles using medicinal plant *Hagenia abyssinica (Brace) JF. Gmel*. leaf extract: antimicrobial properties. J. Nanomater. 2020, 1–12. Available from: https://doi.org/10.1155/2020/3924081.

Murty, B.S., Shankar, P., Raj, B., Rath, B.B., Murday, J., 2013. Tools to characterize nanomaterials. Textbook of Nanoscience and Nanotechnology. Springer Berlin Heidelberg, Berlin, Heidelberg, pp. 149–175. Available from: https://doi.org/10.1007/978-3-642-28030-6_5.

Muthuswamy, S., Rupasinghe, H.P.V., Stratton, G.W., 2008. Antimicrobial effect of cinnamon bark extract on *Escherichia Coli* O157:H7, *Listeria Innocua* And Fresh-Cut Apple Slices: cinnamon as an antimicrobial source For Fresh-cut apples. J. Food Saf. 28, 534–549. Available from: https://doi.org/10.1111/j.1745-4565.2008.00129.x.

Muthu, K., Priya, S., 2017. Green synthesis, characterization and catalytic activity of silver nanoparticles using *Cassia auriculata* flower extract separated fraction. Spectrochim. Acta A Mol. Biomol. Spectrosc. 179, 66–72. Available from: https://doi.org/10.1016/j.saa.2017.02.024.

Nabi, G., Ain, Q.-U.-, Tahir, M.B., Nadeem Riaz, K., Iqbal, T., Rafique, M., et al., 2022. Green synthesis of TiO_2 nanoparticles using lemon peel extract: their optical and photocatalytic properties. Int. J. Environ. Anal. Chem. 102, 434–442. Available from: https://doi.org/10.1080/03067319.2020.1722816.

Nadeem, M., Abbasi, B.H., Younas, M., Ahmad, W., Khan, T., 2017. A review of the green syntheses and antimicrobial applications of gold nanoparticles. Green. Chem. Lett. Rev. 10, 216–227. Available from: https://doi.org/10.1080/17518253.2017.1349192.

Nagajyothi, P.C., Muthuraman, P., Sreekanth, T.V.M., Kim, D.H., Shim, J., 2017. Green synthesis: in-vitro anticancer activity of copper oxide nanoparticles against human cervical carcinoma cells. Arab. J. Chem. 10, 215–225. Available from: https://doi.org/10.1016/j.arabjc.2016.01.011.

Narasaiah, B.P., Mandal, B.K., 2020. Remediationof azo-dyes based Toxicity by agro-waste cotton boll peels mediated palladium nanoparticles. J. Saudi Chem. Soc. 24, 267–281. Available from: https://doi.org/10.1016/j.jscs.2019.11.003.

Narayanan, K.B., Sakthivel, N., 2011. Green synthesis of biogenic metal nanoparticles by terrestrial and aquatic phototrophic and heterotrophic eukaryotes and biocompatible agents. Adv. Colloid Interface Sci. 169, 59–79. Available from: https://doi.org/10.1016/j.cis.2011.08.004.

Nasrollahzadeh, M., Sajadi, S.M., Maham, M., 2015. Green synthesis of palladium nanoparticles using *Hippophae rhamnoides* Linn leaf extract and their catalytic activity for the Suzuki–Miyaura coupling in water. J. Mol. Catal. A: Chem. 396, 297–303. Available from: https://doi.org/10.1016/j.molcata.2014.10.019.

Nasrollahzadeh, M., Sajadi, S.M., Rostami-Vartooni, A., Alizadeh, M., Bagherzadeh, M., 2016. Green synthesis of the Pd nanoparticles supported on reduced graphene oxide using barberry fruit extract and its application as a recyclable and heterogeneous catalyst for the reduction of nitroarenes. J. Colloid Interface Sci. 466, 360–368. Available from: https://doi.org/10.1016/j.jcis.2015.12.036.

Nath, D., Banerjee, P., 2013. Green nanotechnology— a new hope for medical biology. Env. Toxicol. Pharmacol. 36, 997–1014. Available from: https://doi.org/10.1016/j.etap.2013.09.002.

Noruzi, M., Zare, D., Khoshnevisan, K., Davoodi, D., 2011. Rapid green synthesis of gold nanoparticles using *Rosa hybrida* petal extract at room temperature. Spectrochim. Acta A Mol. Biomol. Spectrosc. 79, 1461–1465.

Odeniyi, M.A., Okumah, V.C., Adebayo-Tayo, B.C., Odeniyi, O.A., 2020. Green synthesis and cream formulations of silver nanoparticles of *Nauclea latifolia* (African peach) fruit extracts and evaluation of antimicrobial and antioxidant activities. Sustain. Chem. Pharm. 15, 100197. Available from: https://doi.org/10.1016/j.scp.2019.100197.

Parlinska-Wojtan, M., Kus-Liskiewicz, M., Depciuch, J., Sadik, O., 2016. Green synthesis and antibacterial effects of aqueous colloidal solutions of silver nanoparticles using camomile terpenoids as a combined reducing and capping agent. Bioprocess. Biosyst. Eng. 39, 1213–1223. Available from: https://doi.org/10.1007/s00449-016-1599-4.

Pasca, R.-D., Mocanu, A., Cobzac, S.-C., Petean, I., Horovitz, O., Tomoaia-Cotisel, M., 2014. Biogenic Syntheses of gold nanoparticles using plant extracts. Part. Sci. Technol. 32, 131–137. Available from: https://doi.org/10.1080/02726351.2013.839589.

Patil, C.D., Patil, S.V., Borase, H.P., Salunke, B.K., Salunkhe, R.B., 2012. Larvicidal activity of silver nanoparticles synthesized using *Plumeria rubra* plant latex against Aedes aegypti and Anopheles stephensi. Parasitol. Res. 110, 1815–1822. Available from: https://doi.org/10.1007/s00436-011-2704-x.

Patra, J.K., Kwon, Y., Baek, K.-H., 2016. Green biosynthesis of gold nanoparticles by onion peel extract: synthesis, characterization and biological activities. Adv. Powder Technol. 27, 2204–2213. Available from: https://doi.org/10.1016/j.apt.2016.08.005.

Perveen, K., Husain, F.M., Qais, F.A., Khan, A., Razak, S., Afsar, T., et al., 2021. Microwave-assisted rapid green synthesis of gold nanoparticles using seed extract of *Trachyspermum ammi*: ROS mediated biofilm inhibition and anticancer activity. Biomolecules 11, 197. Available from: https://doi.org/10.3390/biom11020197.

Philip, D., 2011. Mangifera indica leaf-assisted biosynthesis of well-dispersed silver nanoparticles. Spectrochim. Acta A Mol. Biomol. Spectrosc. 78, 327–331. Available from: https://doi.org/10.1016/j.saa.2010.10.015.

Phillip, D., 2009. Biosynthesis of Ag, Au and Au-Ag nanoparticles using edible mushrooms extracts. Spectrochim. Acta A Mol. Biomol. Spectrosc. 73, 374–381.

Ponarulselvam, S., Panneerselvam, C., Murugan, K., Aarthi, N., Kalimuthu, K., Thangamani, S., 2012. Synthesis of silver nanoparticles using leaves of Catharanthus roseus Linn. G. Don and their antiplasmodial activities. Asian Pac. J. Trop. Biomed. 2, 574–580. Available from: https://doi.org/10.1016/S2221-1691(12)60100-2.

Porcel, E., Liehn, S., Remita, H., Usami, N., Kobayashi, K., Furusawa, Y., et al., 2010. Platinum nanoparticles: a promising material for future cancer therapy? Nanotechnology 21, 085103. Available from: https://doi.org/10.1088/0957-4484/21/8/085103.

Prasad, K.S., Prasad, S.K., Ansari, M.A., Alzohairy, M.A., Alomary, M.N., AlYahya, S., et al., 2020. Tumoricidal and bactericidal properties of ZnO NPs synthesized using *Cassia auriculata* leaf extract. Biomolecules 10, E982. Available from: https://doi.org/10.3390/biom10070982.

Prathna, T.C., Chandrasekaran, N., Raichur, A.M., Mukherjee, A., 2011. Biomimetic synthesis of silver nanoparticles by *Citrus limon* (lemon) aqueous extract and theoretical prediction of particle size. Coll. Surf. B: Biointerf 82, 152–159.

Qu, Y., Shen, W., Pei, X., Ma, F., You, S., Li, S., et al., 2017. Biosynthesis of gold nanoparticles by *Trichoderma* sp. WL-Go for azo dyes decolorization. J. Env. Sci. (China) 56, 79–86. Available from: https://doi.org/10.1016/j.jes.2016.09.007.

Rabiee, N., Bagherzadeh, M., Kiani, M., Ghadiri, A.M., 2020. Rosmarinus officinalis directed palladium nanoparticle synthesis: Investigation of potential antibacterial, antifungal and Mizoroki-Heck catalytic activities. Adv. Powder Technol. 31, 1402–1411. Available from: https://doi.org/10.1016/j.apt.2020.01.024.

Rahman, Q.I., Ahmad, M., Misra, S.K., Lohani, M., 2013a. Effective photocatalytic degradation of rhodamine B dye by ZnO nanoparticles. Mater. Lett. 91, 170–174. Available from: https://doi.org/10.1016/j.matlet.2012.09.044.

Rahman, Q.I., Ahmad, M., Misra, S.K., Lohani, M.B., 2013b. Hexagonal ZnO nanorods assembled flowers for photocatalytic dye degradation: growth, structural and optical properties. Superlattices Microstruct. 64, 495–506. Available from: https://doi.org/10.1016/j.spmi.2013.10.011.

Rajakumar, G., Rahuman, A.A., Priyamvada, B., Khanna, V.G., Kumar, D.K., Sujin, P.J., 2012. Eclipta prostrata leaf aqueous extract mediated synthesis of titanium dioxide nanoparticles. Mater. Lett. 68, 115–117. Available from: https://doi.org/10.1016/j.matlet.2011.10.038.

Ramachandiran, D., Elangovan, M., Rajesh, K., 2021. Structural, optical, biological and photocatalytic activities of platinum nanoparticles using salixtetrasperma leaf extract via hydrothermal and ultrasonic methods. Optik 244, 167494. Available from: https://doi.org/10.1016/j.ijleo.2021.167494.

Rambabu, K., Bharath, G., Banat, F., Show, P.L., 2021. Green synthesis of zinc oxide nanoparticles using *Phoenix dactylifera* waste as bioreductant for effective dye degradation and antibacterial performance in wastewater treatment. J. Hazard. Mater. 402, 123560. Available from: https://doi.org/10.1016/j.jhazmat.2020.123560.

Ramesh, P., Rajendran, A., Sundaram, M., 2014. Green synthesis of Zinc oxide nanoparticles using flower extract *Cassia auriculata*. J. Nanosci. Nanotechnol. 2, 41–45.

Rauf, M.A., Ashraf, S.S., 2009. Fundamental principles and application of heterogeneous photocatalytic degradation of dyes in solution. Chem. Eng. J. 151, 10–18. Available from: https://doi.org/10.1016/j.cej.2009.02.026.

Reddy, V., Torati, R.S., Oh, S., Kim, C., 2012. Biosynthesis of gold nanoparticles assisted by *Sapindus mukorossi* gaertn. fruit pericarp and their catalytic application for the reduction of *p*-nitroaniline. Ind. Eng. Chem. Res. 52, 556–564.

Rodríguez-Félix, F., López-Cota, A.G., Moreno-Vásquez, M.J., Graciano-Verdugo, A.Z., Quintero-Reyes, I.E., Del-Toro-Sánchez, C.L., et al., 2021. Sustainable-green synthesis of silver nanoparticles using safflower (*Carthamus tinctorius* L.) waste extract and its antibacterial activity. Heliyon 7, e06923. Available from: https://doi.org/10.1016/j.heliyon.2021.e06923.

Rodríguez-León, E., Rodríguez-Vázquez, B.E., Martínez-Higuera, A., Rodríguez-Beas, C., Larios-Rodríguez, E., Navarro, R.E., et al., 2019. Synthesis of gold nanoparticles using *mimosa tenuiflora* extract, assessments of cytotoxicity, cellular uptake, and catalysis. Nanoscale Res. Lett. 14, 334. Available from: https://doi.org/10.1186/s11671-019-3158-9.

Rolim, W.R., Pelegrino, M.T., de Araújo Lima, B., Ferraz, L.S., Costa, F.N., Bernardes, J.S., et al., 2019. Green tea extract mediated biogenic synthesis of silver nanoparticles: characterization, cytotoxicity evaluation and antibacterial activity. Appl. Surf. Sci. 463, 66–74. Available from: https://doi.org/10.1016/j.apsusc.2018.08.203.

Sai Saraswathi, V., Tatsugi, J., Shin, P.-K., Santhakumar, K., 2017. Facile biosynthesis, characterization, and solar assisted photocatalytic effect of ZnO nanoparticles mediated by leaves of L. speciosa. J. Photochem. Photobiol. B 167, 89–98. Available from: https://doi.org/10.1016/j.jphotobiol.2016.12.032.

Salayová, A., Bedlovičová, Z., Daneu, N., Baláž, M., Lukáčová Bujňáková, Z., Balážová, Ľ., et al., 2021. Green synthesis of silver nanoparticles with antibacterial activity using various medicinal plant extracts: morphology and antibacterial efficacy. Nanomaterials 11, 1005. Available from: https://doi.org/10.3390/nano11041005.

Sanakousar, F.M., Vidyasagar, C.C., Jiménez-Pérez, V.M., Prakash, K., 2022. Recent progress on visible-light-driven metal and non-metal doped ZnO nanostructures for photocatalytic degradation of organic pollutants. Mater. Sci. Semicond. Process. 140, 106390. Available from: https://doi.org/10.1016/j.mssp.2021.106390.

Sastry, A.B.S., Karthik Aamanchi, R.B., Sree Rama Linga Prasad, Ch, Murty, B.S., 2013. Large-scale green synthesis of Cu nanoparticles. Environ. Chem. Lett. 11, 183–187. Available from: https://doi.org/10.1007/s10311-012-0395-x.

Sathishkumar, M., Sneha, K., Yun, Y.-S., 2010. Immobilization of silver nanoparticles synthesized using *Curcuma longa* tuber powder and extract on cotton cloth for bactericidal activity. Bioresour. Technol. 101, 7958–7965. Available from: https://doi.org/10.1016/j.biortech.2010.05.051.

Sathiyavimal, S., Vasantharaj, S., Veeramani, V., Saravanan, M., Rajalakshmi, G., Kaliannan, T., et al., 2021. Green chemistry route of biosynthesized copper oxide nanoparticles using *Psidium guajava* leaf extract and their antibacterial activity and effective removal of industrial dyes. J. Environ. Chem. Eng. 9, 105033. Available from: https://doi.org/10.1016/j.jece.2021.105033.

Sekar, V., Al-Ansari, M.M., Narenkumar, J., Al-Humaid, L., Arunkumar, P., Santhanam, A., 2022. Synthesis of gold nanoparticles (AuNPs) with improved anti-diabetic, antioxidant and anti-microbial activity from *Physalis minima*. J. King Saud. Univ. Sci. 34, 102197. Available from: https://doi.org/10.1016/j.jksus.2022.102197.

Selvam, K., Albasher, G., Alamri, O., Sudhakar, C., Selvankumar, T., Vijayalakshmi, S., et al., 2022. Enhanced photocatalytic activity of novel *Canthium coromandelicum* leaves based copper oxide nanoparticles for the degradation of textile dyes. Environ. Res. 211, 113046. Available from: https://doi.org/10.1016/j.envres.2022.113046.

Selvi, A.M., Palanisamy, S., Jeyanthi, S., Vinosha, M., Mohandoss, S., Tabarsa, M., et al., 2020. Synthesis of Tragia involucrata mediated platinum nanoparticles for comprehensive therapeutic applications: antioxidant, antibacterial and mitochondria-associated apoptosis in HeLa cells. Process. Biochem. 98, 21–33. Available from: https://doi.org/10.1016/j.procbio.2020.07.008.

Shahaby, O.E., 2013. Evaluation of antimicrobial activity of water infusion plant-mediated silver nanoparticles. J. Nanomed. Nanotechol. 04. Available from: https://doi.org/10.4172/2157-7439.1000178.

Shah, I.H., Ashraf, M., Sabir, I.A., Manzoor, M.A., Malik, M.S., Gulzar, S., et al., 2022. Green synthesis and characterization of copper oxide nanoparticles using *Calotropis procera* leaf extract and their different biological potentials. J. Mol. Struct. 1259, 132696. Available from: https://doi.org/10.1016/j.molstruc.2022.132696.

Shankar, S.S., Ahmad, A., Sastry, M., 2003. Geranium leaf assisted biosynthesis of silver nanoparticles. Biotechnol. Prog. 19, 1627–1631. Available from: https://doi.org/10.1021/bp034070w.

Shanker, U., Jassal, V., Rani, M., 2017. Green synthesis of iron hexacyanoferrate nanoparticles: potential candidate for the degradation of toxic PAHs. J. Environ. Chem. Eng. 5, 4108–4120. Available from: https://doi.org/10.1016/j.jece.2017.07.042.

Sharifi-Rad, M., Pohl, P., Epifano, F., Álvarez-Suarez, J.M., 2020. Green synthesis of silver nanoparticles using *Astragalus tribuloides* delile. root extract: characterization, antioxidant, antibacterial, and anti-inflammatory activities. Nanomaterials 10, 2383. Available from: https://doi.org/10.3390/nano10122383.

Sharma, J.K., Akhtar, M.S., Ameen, S., Srivastava, P., Singh, G., 2015. Green synthesis of CuO nanoparticles with leaf extract of Calotropis gigantea and its dye-sensitized solar cells applications. J. Alloy Compd. 632, 321–325. Available from: https://doi.org/10.1016/j.jallcom.2015.01.172.

Sharma, R.K., Gulati, S., Mehta, S., 2012. Preparation of gold nanoparticles using tea: a green chemistry experiment. J. Chem. Educ. 89, 1316–1318. Available from: https://doi.org/10.1021/ed2002175.

Sharma, G., Nim, S., Alle, M., Husen, A., Kim, J.C., 2022. Nanoparticle-mediated delivery of flavonoids for cancer therapy: prevention and treatment. In: Kim, J.C., Alle, M., Husen, A. (Eds.), Smart Nanomaterials in Biomedical Applications. Nanotechnology in the Life Sciences. Springer, Cham, pp. 61–100. Available from: https://doi.org/10.1007/978-3-030-84262-8_3, ISBN: 978-3-030-84261-1.

Sharma, P., Pandey, V., Sharma, M.M.M., Patra, A., Singh, B., Mehta, S., et al., 2021. A review on biosensors and nanosensors application in agroecosystems. Nano Res. Lett. 16, 136. Available from: https://doi.org/10.1186/s11671-021-03593-0.

Sheik Mydeen, S., Raj Kumar, R., Kottaisamy, M., Vasantha, V.S., 2020. Biosynthesis of ZnO nanoparticles through extract from *Prosopis juliflora* plant leaf: antibacterial activities and a new approach by rust-induced photocatalysis. J. Saudi Chem. Soc. 24, 393–406. Available from: https://doi.org/10.1016/j.jscs.2020.03.003.

Shende, S., Ingle, A.P., Gade, A., Rai, M., 2015. Green synthesis of copper nanoparticles by Citrus medica Linn. (Idilimbu) juice and its antimicrobial activity. World J. Microbiol. Biotechnol. 31, 865–873. Available from: https://doi.org/10.1007/s11274-015-1840-3.

Sheny, D.S., Philip, D., Mathew, J., 2013. Synthesis of platinum nanoparticles using dried *Anacardium occidentale* leaf and its catalytic and thermal applications. Spectrochim. Acta A Mol. Biomol. Spectrosc. 114, 267–271. Available from: https://doi.org/10.1016/j.saa.2013.05.028.

Shevchenko, A., Wilm, M., Vorm, O., Mann, M., 1996. Mass spectrometric sequencing of proteins from silver-stained polyacrylamide gels. Anal. Chem. 68, 850–858. Available from: https://doi.org/10.1021/ac950914h.

Siddiqi, K.S., Husen, A., 2016a. Fabrication of metal and metal oxide nanoparticles by algae and their toxic effects. Nanoscale Res. Lett. 11 (363), 1–11. Available from: https://doi.org/10.1186/s11671-016-1580-9.

Siddiqi, K.S., Husen, A., 2016b. Fabrication of metal nanoparticles from fungi and metal salts: scope and application. Nanoscale Res. Lett. 11 (98), 1–15. Available from: https://doi.org/10.1186/s11671-016-1311-2.

Silva Viana, R.L., Pereira Fidelis, G., Jane Campos Medeiros, M., Antonio Morgano, M., Gabriela Chagas Faustino Alves, M., Domingues Passero, L.F., et al., 2020. Green synthesis of antileishmanial and antifungal silver nanoparticles using corn cob xylan as a reducing and stabilizing agent. Biomolecules 10, E1235. Available from: https://doi.org/10.3390/biom10091235.

Singh, G., Babele, P.K., Shahi, S.K., Sinha, R.P., Tyagi, M.B., Kumar, A., 2014. Green synthesis of silver nanoparticles using cell extracts of anabaena doliolum and screening of its antibacterial and antitumor activity. J. Microbiol. Biotechnol. 24, 1354–1367. Available from: https://doi.org/10.4014/jmb.1405.05003.

Singh, R., Hano, C., Nath, G., Sharma, B., 2021. Green biosynthesis of silver nanoparticles using leaf extract of *Carissa carandas* L. and their antioxidant and antimicrobial activity against human pathogenic bacteria. Biomolecules 11, 299. Available from: https://doi.org/10.3390/biom11020299.

Singh, M., Sinha, I., Premkumar, M., Singh, A.K., Mandal, R.K., 2010. Structural and surface plasmon behavior of Cu nanoparticles using different stabilizers. Colloids Surf. Physicochem. Eng. Asp. 359, 88–94. Available from: https://doi.org/10.1016/j.colsurfa.2010.01.069.

Skoog, D.A., West, D.M., Holler, F.J., 1988. Fundamentals of Analytical Chemistry, fifth ed. Saunders College Publishing, New York.

Song, J.Y., Kim, B.S., 2009. Rapid biological synthesis of silver nanoparticles using plant leaf extracts. Bioprocess. Biosyst. Eng. 32, 79–84. Available from: https://doi.org/10.1007/s00449-008-0224-6.

Song, J.Y., Kwon, E.-Y., Kim, B.S., 2010. Biological synthesis of platinum nanoparticles using Diopyros kaki leaf extract. Bioprocess. Biosyst. Eng. 33, 159–164. Available from: https://doi.org/10.1007/s00449-009-0373-2.

Soundarrajan, C., Sankari, A., Dhandapani, P., Maruthamuthu, S., Ravichandran, S., Sozhan, G., et al., 2012. Rapid biological synthesis of platinum nanoparticles using Ocimum sanctum for water electrolysis applications. Bioprocess. Biosyst. Eng. 35, 827–833. Available from: https://doi.org/10.1007/s00449-011-0666-0.

Stan, M., Lung, I., Soran, M.-L., Leostean, C., Popa, A., Stefan, M., et al., 2017. Removal of antibiotics from aqueous solutions by green synthesized magnetite nanoparticles with selected agro-waste extracts. Process. Saf. Environ. Prot. 107, 357–372. Available from: https://doi.org/10.1016/j.psep.2017.03.003.

Subhashini, D., Nachiyar, C.V., 2014. *Albizia saman*: a green route for the reduction of bulk TiO_2. Int. J. Chemtech. Res. 6, 5137–5141.

Suman, T.Y., Rajasree, S.R.R., Ramkumar, R., Rajthilak, C., Perumal, P., 2014. The Green synthesis of gold nanoparticles using an aqueous root extract of *Morinda citrifolia* L. Spectrochim. Acta A Mol. Biomol. Spectrosc. 118, 11–16. Available from: https://doi.org/10.1016/j.saa.2013.08.066.

Sun, Q., Cai, X., Li, J., Zheng, M., Chen, Z., Yu, C.P., 2014. Green synthesis of silver nanoparticles using tea leaf extract and evaluation of their stability and antibacterial activity. Coll. Surf. A: Physicochem. Eng. Asp. 444, 226–231.

Thakar, M.A., Saurabh Jha, S., Phasinam, K., Manne, R., Qureshi, Y., Hari Babu, V.V., 2022. X ray diffraction (XRD) analysis and evaluation of antioxidant activity of copper oxide nanoparticles synthesized from leaf extract of *Cissus vitiginea*. Mater. Today: Proc. 51, 319–324. Available from: https://doi.org/10.1016/j.matpr.2021.05.410.

Thirumurugan, A., Aswitha, P., Kiruthika, C., Nagarajan, S., Christy, A.N., 2016. Green synthesis of platinum nanoparticles using *Azadirachta indica*—An eco-friendly approach. Mater. Lett. 170, 175–178. Available from: https://doi.org/10.1016/j.matlet.2016.02.026.

Thiruvengadam, M., Chung, I.-M., Gomathi, T., Ansari, M.A., Gopiesh Khanna, V., Babu, V., et al., 2019. Synthesis, characterization and pharmacological potential of green synthesized copper nanoparticles. Bioprocess. Biosyst. Eng. 42, 1769–1777. Available from: https://doi.org/10.1007/s00449-019-02173-y.

Tiwari, M., Jain, P., Chandrashekhar Hariharapura, R., Narayanan, K., Bhat, K., U., Udupa, N., et al., 2016. Biosynthesis of copper nanoparticles using copper-resistant Bacillus cereus, a soil isolate. Process. Biochem. 51, 1348–1356. Available from: https://doi.org/10.1016/j.procbio.2016.08.008.

Ullah, S., Ahmad, A., Wang, A., Raza, M., Jan, A.U., Tahir, K., et al., 2017. Bio-fabrication of catalytic platinum nanoparticles and their in vitro efficacy against lungs cancer cells line (A549). J. Photochem. Photobiol. B: Biol. 173, 368–375. Available from: https://doi.org/10.1016/j.jphotobiol.2017.06.018.

Upadhyay, L.S.B., Verma, M., 2014. Synthesis and characterization of cysteine functionalized silver nanoparticles for biomolecule immobilization. Bioprocess. Biosyst. Eng. 37, 2139–2148.

Vijayakumar, S., Arulmozhi, P., Kumar, N., Sakthivel, B., Prathip Kumar, S., Praseetha, P.K., 2020. *Acalypha fruticosa* L. leaf extract mediated synthesis of ZnO nanoparticles: characterization and antimicrobial activities. Mater. Today Proc. 23, 73–80. Available from: https://doi.org/10.1016/j.matpr.2019.06.660.

Vinay, S.P., Udayabhanu, Nagaraju, G., Chandrappa, C.P., Chandrasekhar, N., 2020. Hydrothermal synthesis of gold nanoparticles using spider cobweb as novel biomaterial: application to photocatalytic. Chem. Phys. Lett. 748, 137402. Available from: https://doi.org/10.1016/j.cplett.2020.137402.

Vinodhini, S., Vithiya, B.S.M., Prasad, T.A.A., 2022. Green synthesis of palladium nanoparticles using aqueous plant extracts and its biomedical applications. J. King Saud. Univ. Sci. 34, 102017. Available from: https://doi.org/10.1016/j.jksus.2022.102017.

Vishveshvar, K., Aravind Krishnan, M.V., Haribabu, K., Vishnuprasad, S., 2018. Green synthesis of copper oxide nanoparticles using Ixiro coccinea plant leaves and its characterization. BioNanoScience 8, 554–558. Available from: https://doi.org/10.1007/s12668-018-0508-5.

Xiao, Z., Yuan, M., Yang, B., Liu, Z., Huang, J., Sun, D., 2016. Plant-mediated synthesis of highly active iron nanoparticles for Cr (VI) removal: investigation of the leading biomolecules. Chemosphere 150, 357–364. Available from: https://doi.org/10.1016/j.chemosphere.2016.02.056.

Xu, J., Wilson, A.R., Rathmell, A.R., Howe, J., Chi, M., Wiley, B.J., 2011. Synthesis and catalytic properties of Au-Pd nanoflowers. ACS Nano 5, 6119–6127. Available from: https://doi.org/10.1021/nn201161m.

Yang, L., Watts, D.J., 2005. Particle surface characteristics may play an important role in phytotoxicity of alumina nanoparticles. Toxicol. Lett. 158, 122–132. Available from: https://doi.org/10.1016/j.toxlet.2005.03.003.

Yan, D., Zhang, H., Chen, L., Zhu, G., Wang, Z., Xu, H., et al., 2014. Supercapacitive properties of Mn_3O_4 nanoparticles bio-synthesized from banana peel extract. RSC Adv. 4, 23649. Available from: https://doi.org/10.1039/c4ra02603a.

Yassin, M.T., Mostafa, A.A.-F., Al-Askar, A.A., Al-Otibi, F.O., 2022. Facile green synthesis of silver nanoparticles using aqueous leaf Extract of *origanum majorana* with potential bioactivity against multidrug resistant bacterial strains. Crystals 12, 603. Available from: https://doi.org/10.3390/cryst12050603.

Zangeneh, M.M., Zangeneh, A., 2020. Novel green synthesis of *Hibiscus sabdariffa* flower extract conjugated gold nanoparticles with excellent anti-acute myeloid leukemia effect in comparison to daunorubicin in a leukemic rodent model. Appl. Organomet. Chem. 34. Available from: https://doi.org/10.1002/aoc.5271.

Zhang, G., Liu, Z., Xiao, Z., Huang, J., Li, Q., Wang, Y., et al., 2015. Ni_2 P-graphite nanoplatelets supported Au–Pd core–shell nanoparticles with superior electrochemical properties. J. Phys. Chem. C 119, 10469–10477. Available from: https://doi.org/10.1021/acs.jpcc.5b02107.

Zhang, L., Pornpattananangku, D., Hu, C.-M.J., Huang, C.-M., 2010. Development of nanoparticles for antimicrobial drug delivery. Curr. Med. Chem. 17, 585–594. Available from: https://doi.org/10.2174/092986710790416290.